bioRxiv preprint doi: https://doi.org/10.1101/2021.09.24.461749; this version posted September 25, 2021. The copyright holder for this preprint (which was not certified by peer review) is the author/funder, who has granted bioRxiv a license to display the preprint in perpetuity. It is made available under aCC-BY-NC-ND 4.0 International license.

Cancer missense mutations in the BRC repeats of BRCA2 protein disrupt RAD51 binding and activity leading to chemotherapeutic sensitivity

Judit Jimenez-Sainz, Joshua Mathew, Jennifer Garbarino, Joseph P. Eder, and Ryan B. Jensen

Department of Therapeutic Radiology, Yale University School of Medicine, New Haven, CT

bioRxiv preprint doi: https://doi.org/10.1101/2021.09.24.461749; this version posted September 25, 2021. The copyright holder for this preprint (which was not certified by peer review) is the author/funder, who has granted bioRxiv a license to display the preprint in perpetuity. It is made available under aCC-BY-NC-ND 4.0 International license.

Abstract

BRCA2 is a tumor suppressor gene that maintains genome stability by mediating the high fidelity repair of DNA double-strand breaks (DSBs) through homology-directed repair (HDR). Pathogenic mutations in BRCA2 predispose to breast, ovarian, pancreatic, prostate, and other cancers. Mutations in BRCA2 leading to severe protein truncation predict pathogenicity, however, missense mutations with unknown functional consequences, designated Variants of Uncertain Significance (VUS), comprise 60% of BRCA2 sequence changes deposited in clinical databases. Classifying BRCA2 VUS correctly is critical for relaying clinically actionable information to patients concerning future cancer risk or current treatment options. In this study, we identified and biochemically characterized three BRCA2 VUS located in BRC repeats to determine the impact on canonical HDR functions. Two of the germline variants, S1221P and T1980I, map to conserved residues in BRC2 and BRC7, disrupt RAD51 binding, and are diminished in their ability to stabilize RAD51-ssDNA complexes. We provide supporting cellular evidence that S1221P and T1980I are significantly compromised in their response to chemotherapeutics and ionizing radiation. The third variant, T1346I, lies within the spacer region between BRC2 and BRC3 but remains fully functional. We conclude that T1346I has a neutral impact on BRCA2 function, while S1221P and T1980I are hypomorphic alleles that disrupt the ability of BRCA2 to fully engage and stabilize RAD51 nucleoprotein filaments.

bioRxiv preprint doi: https://doi.org/10.1101/2021.09.24.461749; this version posted September 25, 2021. The copyright holder for this preprint (which was not certified by peer review) is the author/funder, who has granted bioRxiv a license to display the preprint in perpetuity. It is made available under aCC-BY-NC-ND 4.0 International license.

Conclusions/Highlights

- The BRCA2 missense variants, S1221P in BRC2 and T1980I in BRC7, are hypomorphic alleles which exhibit multiple defects in response to chemotherapeutics, DNA damage, and cellular stress.
- The biochemical defects in S1221P and T1980I include disruption of RAD51 binding and failure to stimulate RAD51-ssDNA complex formation.
- Identification of a tumor derived somatic BRCA2 missense mutation in the spacer region between BRC2 and BRC3, T1346I, is a benign variant.

Potential Limitations

- Given that BRCA2 plays several roles in cellular function, it is possible that the VUS studied disrupt BRCA2 function in ways not measured by the assays described here.
- Therefore, further experimentation is necessary to validate the observed functionality of the variants studied and discern partial loss of function variants from fully neutral or pathogenic ones.
- Overexpression of the *BRCA2* cDNA may underestimate the functional effect of some variants. However, it is feasible that cDNA-based overexpression of these variants can partially rescue HR and other BRCA2 functions.
- Caution is warranted when interpreting results from an assay focusing on a single specific biochemical activity to predict pathogenicity of BRCA2. This is extremely challenging for proteins with multiple biochemical and biological functions such as BRCA2. Up to date a small number of pathogenic or non-pathogenic variants have been evaluated and based on. Therefore,

bioRxiv preprint doi: https://doi.org/10.1101/2021.09.24.461749; this version posted September 25, 2021. The copyright holder for this preprint (which was not certified by peer review) is the author/funder, who has granted bioRxiv a license to display the preprint in perpetuity. It is made available under aCC-BY-NC-ND 4.0 International license.

discriminating a true intermediate function variant from a neutral or fully pathogenic variant remains difficult and integration of multiple functional assays may be necessary as the presented in this study.

Introduction

BRCA2 (BReast CAncer type 2 susceptibility gene) is a mediator protein that stimulates homology-directed repair (HDR) of DNA double-strand breaks (DSBs) via RAD51-dependent DNA strand invasion, pairing, and exchange (Jensen et al., 2010; Scully and Livingston, 2000; Venkitaraman, 2002). Mechanistically, BRCA2 binds and loads RAD51 onto ssDNA generated by strand resection. BRCA2 directs RAD51 onto single-stranded DNA (ssDNA) while limiting binding to double-stranded DNA (dsDNA), downregulates the ATPase activity of RAD51, and displaces Replication Protein A (RPA) from ssDNA (Jensen *et al.*, 2010; Liu et al., 2010; Thorslund et al., 2007). Loss of BRCA2 in human cells leads to severe defects in HDR, genomic instability, spontaneous micronuclei formation, diminished fork protection following replication stress, impaired RAD51 foci formation in response to DNA damage, and sensitivity to chemotherapeutics such as platinum agents and PARP inhibitors (PARPi) (Abul-Husn et al., 2019; Chen et al., 1999; Chen et al., 1998; Moynahan et al., 2001; Patel et al., 1998).

To date, four key domains in BRCA2 have emerged from both sequence based and structural studies (**Figure 1A**): an N-terminal region, eight BRC repeats located in the middle of the protein, an alpha helices region and three tandem oligonucleotide/oligosaccharide-binding folds (OB-folds) termed the DNA binding domain (DBD), and the C-terminal domain (CTD) (Bignell et al., 1997; McAllister et al., 1997; Yang *et al.*, 2002)The eight BRC repeats located in the middle of BRCA2 interact with RAD51 and distinct functions have been ascribed to each of two modules: BRC1-4 and BRC5-8 (Carreira and Kowalczykowski, 2011; Chatterjee et al.,

bioRxiv preprint doi: https://doi.org/10.1101/2021.09.24.461749; this version posted September 25, 2021. The copyright holder for this preprint (which was not certified by peer review) is the author/funder, who has granted bioRxiv a license to display the preprint in perpetuity. It is made available under aCC-BY-NC-ND 4.0 International license.

2016). The BRC1-4 module binds free monomeric RAD51 while BRC5-8 binds RAD51 only when assembled onto ssDNA (Carreira and Kowalczykowski, 2011; Chatterjee *et al.*, 2016). The DBD of BRCA2 has been shown to bind DSS1, ssDNA, and presumably dsDNA as well (Yang *et al.*, 2002). The CTD (also known as TR2) binds RAD51 only when complexed with ssDNA as a nucleoprotein filament (similar to BRC5-8) and RAD51 filament binding is regulated by phosphorylation at the S3291 residue (Carreira et al., 2009; Carreira and Kowalczykowski, 2011; Chatterjee *et al.*, 2016; Chen *et al.*, 1998; Esashi et al., 2007; Mizuta et al., 1997; Pellegrini et al., 2002; Sharan et al., 1997; Wong et al., 1997).

Nonsense mutations in BRCA2 that lead to protein truncation immediately predict pathogenicity as deletion of the DBD would impair key HDR functions, and perhaps more importantly, deletion of nuclear localization signals (NLSs) at the very C-terminus of BRCA2 would result in mislocalization to the cytoplasm (Spain et al., 1999). However, an estimated 80% of germline and somatic mutations identified in patients are missense leading to the substitution of a single amino acid in the full-length protein (Data extracted from ClinVar and cBioPortal from Cancer Genomics, accessed April 2021) (Jimenez-Sainz and Jensen, 2021). Missense mutations often have unknown impacts on function and/or disease linkage and are referred to as Variants of Uncertain Significance (VUS). With respect to counseling for future cancer risk, germline VUS findings often lack genetic linkage data. VUS are likely to be unique to individual families, and thus, in the absence of any functional insight, make clinical management of these patients extremely challenging. In a search of the ClinVar database, more than 60% of the total identified BRCA2 mutations were VUS (Jimenez-Sainz and Jensen, 2021). Notably, the majority of the 1,388 missense mutations reported within the BRC repeats domain of BRCA2 are classified as VUS (Data extracted from ClinVar accessed April 2021) (Jimenez-Sainz and Jensen, 2021).

The critical role of the BRC repeats in binding, loading, and stabilizing RAD51 on ssDNA prompted us to study the functionality of variants in this domain. Moreover, we lack

bioRxiv preprint doi: https://doi.org/10.1101/2021.09.24.461749; this version posted September 25, 2021. The copyright holder for this preprint (which was not certified by peer review) is the author/funder, who has granted bioRxiv a license to display the preprint in perpetuity. It is made available under aCC-BY-NC-ND 4.0 International license.

understanding surrounding the biochemical impact of missense mutations in a single BRC repeat, or between repeats, within the context of the full-length BRCA2 protein. We focused on two variants located within the BRC2 and BRC7 repeats, S1221P and T1980I respectively. As these two amino acid substitutions are situated within a conserved RAD51 binding core motif, we predicted RAD51 interactions and regulation by BRCA2 would be disrupted. A third variant, T1346I, located in the spacer region between BRC2 and BRC3 was found in a patient undergoing treatment at the Yale Cancer Center (Lo et al., 2003; Olopade et al., 2003; Tal et al., 2009). The variants were previously deposited in ClinVar lacking clinical interpretation and classified as VUS (https://www.ncbi.nlm.nih.gov/clinvar/variation/51501/, https://www.ncbi.nlm.nih.gov/clinvar/variation/455896/, https://www.ncbi.nlm.nih.gov/clinvar/variation/993173/).

Our findings reveal that missense variants in a single BRC repeat indeed have profound consequences on BRCA2 HDR protein activities that fail to be compensated for by the remaining seven BRC repeats. Altered functions of S1221P and T1980I include impaired cellular response to chemotherapeutics and diminished RAD51 foci formation upon ionizing radiation DNA damage. We provide unique biochemical evidence that S1221P and T1980I disrupt the ability of the BRC repeats to stabilize RAD51-ssDNA complexes, and as a result, stimulation of RAD51-mediated DNA strand exchange activity is reduced. In contrast, T1346I, located between BRC2 and BRC3 repeats, is likely benign as HDR functions were intact and this variant behaved like the wild type BRCA2.

Importance of this study:

Prior studies investigating BRCA2 VUS functionality have been limited by the extent to which characterization was performed, or the inability to purify the full-length protein for biochemical analysis. In this work, we systematically examine BRCA2 functions using both biochemical and genetic means to determine how variants in the BRC domain can impact

bioRxiv preprint doi: https://doi.org/10.1101/2021.09.24.461749; this version posted September 25, 2021. The copyright holder for this preprint (which was not certified by peer review) is the author/funder, who has granted bioRxiv a license to display the preprint in perpetuity. It is made available under aCC-BY-NC-ND 4.0 International license.

canonical HDR and chemosensitivity. The ability to differentiate pathogenic from benign VUS, supported by both cellular and biochemical data, will facilitate future integration of functional assays with genetic linkage and epidemiological data. Achieving this precision medicine goal could one day provide clinically actionable information to patients harboring rare BRCA2 VUS.

Materials and Methods

Sequence alignment and molecular modeling of BRC repeats

BRCA2 amino acids sequences from 9 different organisms were obtained from Uniprot Knowledgebase database http:/www.uniprot.org/ (Consortium, 2011). Alignments were done with ClustalIX (Larkin et al., 2007) http://www.ch.embnet.org/software/ClustalW.html, and Bioedit http/www.mbio.ncsu.edu/BioEdit/biioedit/html (Hall, 1999). Snapgene software was used for BRC2, BRC4 and BRC7 sequence alignment (>60% threshold for shading). The UniprotKB codes of the sequences from different organisms used were: **P51587** *Homo sapiens (Human)***;** Q**9W157** *Drosophila melanogaster (Fruit fly);* **P97929** *Mus musculus (Mouse);* **Q864S8** *Felis catus (Cat);* **O35923** *Rattus norvegicus (Rat);* **A5A3F7** *Strongylocentrotus purpuratus (Purple sea urchin);* **A4ZZ89** *Monodelphis domestica (Gray short-tailed opossum);* **Q8MKI9** *Canis lupus familiaris (Dog) (Canis familiaris);* **A4ZZ90** *Xenopus tropicalis (Western clawed frog) (Silurana tropicalis).*

Swiss-Model Expasy server was used to model BRC2 and BRC7 against BRC4 in the PDB structure 1N0W (Pellegrini *et al.*, 2002; Waterhouse et al., 2018). The modeled BRC2 and BRC7 structures had QMEAN Z-scores greater than -4 (0.06 and -1.42 respectively) and were considered good quality models.

The PyMOL Molecular Graphics System, Version 1.3 Schrödinger, LLC. was then used to visualize the BRC repeat aligned with the 1N0W structure to look at predicted interactions with RAD51. BRC residues were mutated using the mutagenesis tool and rotamers with a frequency

bioRxiv preprint doi: https://doi.org/10.1101/2021.09.24.461749; this version posted September 25, 2021. The copyright holder for this preprint (which was not certified by peer review) is the author/funder, who has granted bioRxiv a license to display the preprint in perpetuity. It is made available under aCC-BY-NC-ND 4.0 International license.

score greater than 10% were analyzed and the least number of clashes were visualized.

Constructs

Point mutations S1221P (3663bp), T1346I (4038bp) and T1980I (5940bp) were cloned into the pBluescript BRCA2 (1-5286 bp) and pUC57 BRCA2 (2141-9117 bp) sequences, respectively, via site-directed mutagenesis. The BRCA2 segments were then subcloned into the phCMV1 mammalian expression vector using NotI and EcoRV restriction enzymes for the S1221P and T1346I insert and SbfI and AgeI for the T1980I insert. We verified the putative recombinant clones through restriction digestion and sequencing analysis. The previously described 2XMBP tag (Jensen *et al.*, 2010) was placed in-frame at the N-terminus of all proteins separated by an Asparagine linker and the PreScission Protease cleavage sequence.

Cell culture

All culture media were supplemented with 10% fetal bovine serum (FBS). HEK293T cells were cultured in DMEM (source (Jensen *et al.*, 2010)); DLD1 cells were cultured in RPMI. Transient transfections were carried out with Turbofect (Thermo Scientific) (2 µg of DNA, 6 well plate) and in HEK293T cells and with JetOptimus (Polyplus Transfection) in DLD1 cells following manufacture's protocol. Calcium Phosphate (25 µg of DNA, 15 cm^2 plate, see BRCA2 purification section) was used in large scale in HEK293T cells (Jensen *et al.*, 2010). All cell lines were tested regularly for mycoplasma (Mycoalert, Lonza)

Generation of stable cell lines

Human colorectal adenocarcinoma DLD-1 $BRCA2^{-/-}$ cells (Horizon Discovery, originally generated by (Hucl et al., 2008)) were stably transfected with 2 µg of DNA using Lipofectamine3000 (Invitrogen). After 48 hours, the cells were trypsinized and diluted 1:2, 1:4, and 1:8 into 100 mm plates containing 1 mg/mL G418. Single cell colonies were picked into 96-

bioRxiv preprint doi: https://doi.org/10.1101/2021.09.24.461749; this version posted September 25, 2021. The copyright holder for this preprint (which was not certified by peer review) is the author/funder, who has granted bioRxiv a license to display the preprint in perpetuity. It is made available under aCC-BY-NC-ND 4.0 International license.

well plates and subsequently cultured into 24-well plates, 12-well plates, and 6-well plates. Positive clones were isolated, and protein expression was detected by western blot and immunofluorescence analyses.

Western blots and amylose pulldowns

Human embryonic kidney HEK293T cells 70% confluent in 6 well plates were transiently transfected with 0.5 µg or 1 µg of the phCMV1 mammalian expression vector containing a 2XMBP fusion to the full-length or partial cDNA of BRCA2, respectively using TurboFect reagent (Thermo Scientific) (Jensen *et al.*, 2010). 0.5 µg of 2XMBP empty construct was transfected into these cells and an untransfected well was also seeded as a negative control. The cells were lysed 48 hours after transfection in 100 µL of lysis buffer: 50 mM HEPES (pH 7.5), 250 mM NaCl, 5 mM EDTA, 1% Igepal CA-630, 3 mM $MgCl_2$, 10 mM DTT and protease inhibitor cocktail (Roche). Cell extracts were batch bound to amylose resin (NEB) for 2 hours to capture the 2XMBP tagged BRCA2 proteins. Total cellular lysate aliquots were taken before batch binding for control analysis. Total cellular lysates and amylose pulldown samples were run on a 4-15% gradient SDS-PAGE TGX stain-free gel (Bio-Rad 456-8086), which was subsequently transferred to an Immobilon-P membrane (Merck Millipore IPVH00010) in 1X Tris/glycine buffer (diluted from 10X Tris/glycine buffer, Bio-Rad 161-0771). The membrane was blocked in 5% milk in 1X TBS-T (diluted from 10X TBS-T: 0.1 M Tris base, 1.5 M NaCl, 0.5% Tween-20). Washes and antibody incubations were done with 1X TBS-T. Primary mouse antibodies against MBP (NEB E8032L, 1:5000) and RAD51 (Novus Biologicals 14b4, 1:1000) and primary rabbit antibody against BRCA2 (Abcam, ab27976) were used for western blotting. Membranes were then incubated with secondary mouse and rabbit antibodies (HRP-conjugated, Santa Cruz Biotechnology sc-516102 and sc-2004, respectively). Protein expression was visualized by incubating with Clarity Western ECL substrate (Bio-Rad 170-5061) for three minutes and

bioRxiv preprint doi: https://doi.org/10.1101/2021.09.24.461749; this version posted September 25, 2021. The copyright holder for this preprint (which was not certified by peer review) is the author/funder, who has granted bioRxiv a license to display the preprint in perpetuity. It is made available under aCC-BY-NC-ND 4.0 International license.

scanning with a ChemiDoc MP imaging system (Bio-Rad). For amylose pull-down assays in DLD1 stable cell lines 3X 15 cm plates were used.

BRC2, BRC7, BRC2-S1221P and BRC7-T1980I synthetic peptides (see table below for amino acid sequences) were ordered from Pierce, resuspended in BRCA2 purification buffer with 150 mM NaCl, 50 mM HEPES pH 8.2, 0.5 mM EDTA, 10% Glycerol, 1 mM DTT. *In vitro* amylose pull-down assays were performed in binding buffer 'B': 50 mM HEPES (pH 7.5), 250 mM NaCl, 0.5 mM EDTA, and 1 mM DTT. Purified 2XMBP fusion proteins (2 µg) were incubated with 1 µg purified RAD51 for 30 minutes at 37 °C and then batch bound to 30 µL of amylose resin for one hour at 4 °C. The complexes were washed with buffer B containing 0.5% Igepal CA-630/0.1% Triton X-100, eluted with 30 µL of 10 mM maltose in buffer B, laemmli sample buffer was added, samples were heated at 54 °C for 4 minutes, and loaded onto a 4-15% gradient SDS-polyacrylamide gel (Bio-Rad TGX Stain-Free gel). The gel was run for 1 hour at 130 Volts. The proteins were visualized in the Stain-Free gel on a ChemiDoc MP imaging system (Bio-Rad). RAD51 protein was visualized by staining with SyproOrange (Invitrogen). The Stain-Free protein bands were quantified using Image Lab software (Bio-Rad).

For competition assays, synthetic BRC peptides were pre-incubated with RAD51 for 30 minutes. In parallel, 2XMBP fusion proteins from HEK293T cells were amylose pulldown for 30 minutes as described above. The 2XMBP proteins bound to amylose beads were washed with buffer B containing 1 M NaCl to disrupt any protein interaction to 2XMBP proteins and buffer B. Subsequent steps were followed as described previously.

PEPTIDES	AMINOACID SEQUENCES
BRC2	NEVGFRGFYSAHGTKLNVSTEALQKAVKLFSDIEN
BRC2-S1221P	NEVGFRGFY**P**AHGTKLNVSTEALQKAVKLFSDIEN
BRC7	SANTCGIFSTASGKSVQVSDASLQNARQVFSEIED
BRC7-T1980I	SANTCGIFS**I**ASGKSVQVSDASLQNARQVFSEIED

bioRxiv preprint doi: https://doi.org/10.1101/2021.09.24.461749; this version posted September 25, 2021. The copyright holder for this preprint (which was not certified by peer review) is the author/funder, who has granted bioRxiv a license to display the preprint in perpetuity. It is made available under aCC-BY-NC-ND 4.0 International license.

Immunofluorescence imaging

Stable cell clones generated from DLD-1 BRCA2$^{-/-}$ cells were grown on coverslips at 10^5 cells/well in a 24-well plate for 24 hours. Cells were washed twice with 1X PBS, fixed in 1% paraformaldehyde-2% sucrose in 1X PBS from 15 minutes at room temperature, washed twice with 1X PBS, permeabilized with methanol for 30 minutes at -20 °C, then washed two more times with 1X PBS, and finally incubated with 0.5% triton in PBS for 10 minutes. Samples were then blocked with 5% BSA in 1X PBS for 30 minutes at room temperature followed by subsequent incubation with primary antibodies against MBP (NEB E8032L, 1:200) and RAD51 (Proteintech 14961-1-AP, 1:100 or Abcam ab63801) in 5% BSA-0.05% TritonX-100 at 4 °C overnight. The next day, cells were washed three times with 1X PBS and incubated with goat anti-rabbit and anti-mouse secondary antibodies conjugated to the fluorophores Alexa-488 and Alexa-546 (Thermo Fisher Scientific A11034 and A11003, respectively; 1:1000). Coverslips were washed three times with 1X PBS, incubated with 30 nM DAPI for 5 minutes and mounted on slides with FluorSave reagent (Calbiochem 345789). Immunofluorescence images were taken using a Keyence BZ-X800E All-in-One Fluorescent Microscope with a 40x or 60x objective lens. Cells were either untreated as control or irradiated at 12 Gy using an X-Rad 320 Biological Irradiator and cells were collected at 6 and 30 hours post irradiation for immunofluorescence protocol.

Clonogenic survival assay

Stable cell clones generated from DLD-1 BRCA2$^{-/-}$ cells were serially diluted and seeded into 6-well plates at concentrations of 100 and 500 cells per well in triplicate for plating efficiency. Simultaneously, cells were seeded for treatment in 6-well plates at 1,000 and 10,000 cells per well in triplicate per treatment dosage. 24 hours after seeding, cells were treated with indicated doses of Mitomycin C (1.5 mM stock in water) Cisplatin (100 mM stock in DMSO) for 1 hr in serum-free media and Olaparib (50 mM stock in DMSO) or BMN (10 nM stock in DMSO) for

bioRxiv preprint doi: https://doi.org/10.1101/2021.09.24.461749; this version posted September 25, 2021. The copyright holder for this preprint (which was not certified by peer review) is the author/funder, who has granted bioRxiv a license to display the preprint in perpetuity. It is made available under aCC-BY-NC-ND 4.0 International license.

durations of 24 hours. Following treatment, media was aspirated, and cells were washed with 1X PBS and re-fed with fresh media containing FBS. Cells were cultured for 14 days to allow colony formation, after which they were stained with crystal violet staining solution (0.25% crystal violet, 3.5% formaldehyde, 72% methanol). Colonies containing 50 or more cells were scored and surviving fractions were determined.

EdU labeling

Stable cell clones generated from DLD-1 BRCA2$^{-/-}$ cells were grown on coverslips at 10^5 cells/well in a 24-well plate for 24 hours. Cells were treated with or irradiated at 12Gy using an X-RAD 320 Biological Irradiator and labeled with 10 µM EdU for 5 hr. After 5 hr of incubation, cells were fixed in 3.7% paraformaldehyde in 1X PBS from 15 minutes at room temperature, washed twice with 3% BSA in 1X PBS, incubated with 0.5% triton in 1x PBS for 20 minutes. Samples were washed with 3% BSA in 1X PBS twice for 5 minutes at room temperature and incubated with Click-iT reaction cocktail (preparation followed manufacture protocol Thermo Fisher Scientific) for 30 minutes at room temperature protected from light. Cells were washed with 1X PBS and incubated with 1x Hoechst 33342 for 10 minutes at room temperature protected from light. Finally, cells were washed twice with 1X PBS and mounted on slides with FluorSave reagent (Calbiochem 345789). Immunofluorescence images were taken using a Keyence BZ-X800E All-in-One Fluorescent Microscope with a 40x or 60x objective lens. Quantification of positive cells (green nuclei) was performed with Cell profiler software following counting and scoring pipeline and percentage of positive cells was represented with Graph Pad version 9.

Protein purification

2XMBP- BRC2, BRC7, S1221P-BRC2, T1980I-BRC7 or BRCA2 wild-type, S1221P, T1346I and T1980I (see table below for amino acid sequences) were purified as described for the

bioRxiv preprint doi: https://doi.org/10.1101/2021.09.24.461749; this version posted September 25, 2021. The copyright holder for this preprint (which was not certified by peer review) is the author/funder, who has granted bioRxiv a license to display the preprint in perpetuity. It is made available under aCC-BY-NC-ND 4.0 International license.

purification full-length BRCA2 protein (Jensen *et al.*, 2010; Lahiri and Jensen, 2021). The phCMV1 constructs with human BRCA2 cDNA and 2XMBP tag was transiently transfected

CONSTRUCTS	AMINO ACID SEQUENCE
2xMBP BRC2	YLTDENEVGFRGFYSAHGTKLNVSTEALQKAVKLFSDIENISEETSAEVHPISL*
2xMBP BRC2-S1221P	YLTDENEVGFRGFY**P**AHGTKLNVSTEALQKAVKLFSDIENISEETSAEVHPISL*
2xMBP BRC4	RDEKIKEPTLLGFHTASGKKVKIAKESLDKVKNLFDEKEQGTSEI*
2xMBP BRC4-T1526A	RDEKIKEPTLLGFH**A**ASGKKVKIAKESLDKVKNLFDEKEQGTSEI*
2xMBP BRC7	GKLHKSVSSANTCGIFSTASGKSVQVSDASLQNARQVFSEIEDSTKQ*
2xMBP BRC7-T1980I	GKLHKSVSSANTCGIFS**I**ASGKSVQVSDASLQNARQVFSEIEDSTKQ*

using $CaPO_4$ precipitation into HEK293T cells, which were harvested 30 hours post-transfection. Cell extracts were batch bound to amylose resin overnight. Bound proteins tagged with 2XMBP were eluted with 100 mM maltose and 8 mM glucose, loaded onto a HiTrap Q column, and step eluted at 450 mM NaCl. Fractions with the greatest 2XMBP BRCA2 concentration were selected for use in further analyses. Subsequent selected fractions were combined and enriched with an Amicon Pro Purification system (10 kDa, Millipore) for use as concentrated BRCA2 samples. All samples were stored at -80 °C. Purified proteins were visualized on a 4-15% gradient SDS-PAGE TGX stain-free gel (Bio-Rad 456-8086) and then stained with Coomassie blue (Bio-Rad 1610786). Protein preparations were quantified by running varying levels of protein on a stain-free gel and quantifying band intensity with Bio-Rad Image Lab software. Samples were also quantified at an absorbance of 280 nm using a NanoDrop spectrophotometer.

RPA and RAD51 were purified as described previously (Anand et al., 2018; Subramanyam and Spies, 2018).

bioRxiv preprint doi: https://doi.org/10.1101/2021.09.24.461749; this version posted September 25, 2021. The copyright holder for this preprint (which was not certified by peer review) is the author/funder, who has granted bioRxiv a license to display the preprint in perpetuity. It is made available under aCC-BY-NC-ND 4.0 International license.

Oligonucleotides	Sequence
RJ-167-mer	5′-CTG CTT TAT CAA GAT AAT TTT TCG ACT CAT CAG AAA TAT CCG TTT CCT ATA TTT ATT CCT ATT ATG TTT TAT TCA TTT ACT TAT TCT TTA TGT TCA TTT TTT ATA TCC TTT ACT TTA TTT TCT CTG TTT ATT CAT TTA CTT ATT TTG TAT TA TCC TTA TCT TAT TTA-3′
RJ-5'Tail-167mer	5'-ATT TAT TCT ATT CCT CTT TAT TTT CTC TGT TTA TTC ATT TAC TTA TTT TGT ATT AAT TTC CTA TAT TTT TTA CTT GTA TTT CTT ATT CAT TTA CTT ATT TTG TAT TAT CCT TAT TTA TAT CCT TTC TGC TTT ATC AAG ATA ATT TTT CGA CTC ATC AGA AAT ATC CG-3'
RJ-167-mer complementary	5'-TAA ATA AGA TAA GGA TAA TAC AAA ATA AGT AAA TGA ATA AAC AGA GAA AAT AAA GTA AAG GAT ATA AAA AAT GAA CAT AAA GAA TAA GTA AAT GAA TAA AAC ATA ATA GGA ATA AAT ATA GGA AAC GGA TAT TTC TGA TGA GTC GAA AAA TTA TCT TGA TAA AGC AG-3'
RJ-PHIX-42-1	5′-CGG ATA TTT CTG ATG AGT CGA AAA ATT ATC TTG ATA AAG CAG-3′

Electrophoretic mobility shift assay

RAD51 (10 nM) was preincubated with 2XMBP BRC2, BRC2-S1221P, BRC7 and BRC7-T1980I peptides at the indicated concentrations (0, 0.25, 0.5, 1, 2 μM) for 15 min, followed by addition of ssDNA (Oligo dT40 labeled with ^{32}P at the 5'end, 400 pM) in buffer 25 mM TrisOAc (pH 7.5), 10 mM $MgCl_2$, 2 mM $CaCl_2$, 0.1 μg/μL BSA, 2 mM ATP, and 1 mM DTT. The mixture was incubated 45min at 37 °C, as indicated.

The following oligonucleotides were utilized to test BRCA2 WT and T1980I full-length binding: RJ-167-mer and RJ-5'Tail-167mer were radiolabeled with ^{32}P at the 5′-end using T4 Polynucleotide Kinase (NEB). To generate the 3′ tail and dsDNA DNA substrates, RJ-167-mer and RJ-167-mer complementary were annealed at a 1:1 molar ratio to RJ-PHIX-42-1, respectively. To generate the 5′ tail DNA substrate, RJ-5'Tail-167mer was annealed at a 1:1 molar ratio to RJ-PHIX-42-1.

2XMBP BRCA2 wild-type and T1980I proteins were incubated at the indicated concentrations with 400 pM of the radiolabeled DNA substrate for 30 minutes at 37 °C. The reactions were resolved by electrophoresis on a 6% polyacrylamide gel in TAE (40 mM Tris–acetate [pH 7.5], 0.5 mM EDTA) buffer for 90 minutes at 80 Volts. The gel was then dried onto

bioRxiv preprint doi: https://doi.org/10.1101/2021.09.24.461749; this version posted September 25, 2021. The copyright holder for this preprint (which was not certified by peer review) is the author/funder, who has granted bioRxiv a license to display the preprint in perpetuity. It is made available under aCC-BY-NC-ND 4.0 International license.

DE81 paper and exposed to a PhosphorImager screen overnight. The screen was scanned on a Molecular Dynamics Storm 840 PhosphorImager and bands were quantified using ImageLab software. The percentage of protein-DNA complexes was calculated as the free radiolabeled DNA remaining in each lane relative to the protein-free lane, which defined the value of 0% complex, or 100% free DNA.

Biotin DNA Pulldowns

The 2XMBP-BRC purified proteins (80 nM) were incubated with 0, 50 or 100 nM of purified RAD51 for 10 minutes at 37 °C in Buffer 'S': 25 mM TrisOAc (pH 7.5), 1 mM $MgCl_2$, 2 mM $CaCl_2$, 0.1 µg/µL BSA, 2 mM ATP, and 1 mM DTT. Then 1 nM of the biotinylated ssDNA was added for 10 minutes at 37 °C . The ssDNA oligonucleotide substrate, RJ-167-mer, was synthesized with a 5' biotin modification and PAGE purified by IDT (Ultramer). Final volumes were normalized with storage buffer as needed. The DNA-protein complexes were then captured by adding 2.5 µL of pre-washed MagnaLink Streptavidin magnetic beads (SoluLink) in buffer SW (Buffer S supplemented with 0.1% Igepal CA-630 and 0.5% Triton X-100). The bead-DNA-protein complexes were rotated at 25 °C for 5 minutes and then washed 3X with buffer SW (lacking 2 mM ATP), resuspended in 20 µL laemmli sample buffer, heated at 54 °C for 4 minutes, and loaded onto a 4-15% gradient SDS-PAGE gel. The amount of RAD51 protein bound and eluted from the biotinylated DNA was determined by western blot using a monoclonal antibody specific to human RAD51 (14B4, Novus).

DNA strand exchange

All DNA substrates were obtained PAGE purified from IDT. The 3' tail DNA substrate was generated by annealing RJ-167-mer to RJ-PHIX-42-1 at a 1:1 molar ratio. The dsDNA donor was generated by first radiolabeling RJ-Oligo1 (5'-TAA TAC AAA ATA AGT AAA TGA ATA AAC AGA

bioRxiv preprint doi: https://doi.org/10.1101/2021.09.24.461749; this version posted September 25, 2021. The copyright holder for this preprint (which was not certified by peer review) is the author/funder, who has granted bioRxiv a license to display the preprint in perpetuity. It is made available under aCC-BY-NC-ND 4.0 International license.

GAA AAT AAA G-3') with ^{32}P (T4 Polynucleotide Kinase) on the 5'-end and annealing it to RJ-Oligo2 (5'-CTT TAT TTT CTC TGT TTA TTC ATT TAC TTA TTT TGT ATT A-3') at a 1:1 molar ratio. The assay buffer contained: 25 mM TrisOAc (pH 7.5), 1 mM $MgCl_2$, 2 mM $CaCl_2$, 0.1 µg/µL BSA, 2 mM ATP, and 1 mM DTT. All pre-incubations and reactions were at 37 °C. The DNA substrates and proteins were at the following concentrations unless otherwise indicated in the figure legend: RPA (0.1 µM); RAD51 (0.4 µM); 3' tail (4 nM molecules); and dsDNA (4 nM molecules). The 3' tail DNA was incubated first with RPA for 5', followed by the addition of BRCA2 WT or T1980I proteins and RAD51, and finally, the radiolabeled donor dsDNA was added for 30 minutes. Where proteins were omitted, storage buffer was substituted. The reaction was terminated with Proteinase K/0.5% SDS for 10 minutes. The reactions were loaded on a 6% polyacrylamide gel in TAE buffer and electrophoresis was at 60 V for 80 minutes. The gel was then dried onto DE81 paper and exposed to a PhosphorImager screen overnight. The percentage of DNA strand exchange product was calculated as labeled product divided by total labeled input DNA in each lane (for further details (Jensen *et al.*, 2010; Lahiri and Jensen, 2021)).

Results

BRCA2 missense variants S1221P and T1980I are predicted to disrupt BRC folding and RAD51 binding.

The eight BRC repeats located in the middle of the BRCA2 protein sequence (**Figure 1A**) mediate important and distinct RAD51 binding functions (Carreira and Kowalczykowski, 2011; Chatterjee *et al.*, 2016; Lo *et al.*, 2003; Wong *et al.*, 1997). Searching the ClinVar database, we identified two potentially pathogenic missense variants, S1221P and T1980I, located in BRC2 and BRC7 respectively (Figure 1A), and classified as VUS or simply described as "not yet reviewed". S1221P and T1980I were mentioned briefly in prior publications as tumor-associated but detailed information regarding their biochemical functionality was not described (Lo *et al.*, 2003; Tal *et al.*, 2009). In addition, we identified a T1346I variant as a

bioRxiv preprint doi: https://doi.org/10.1101/2021.09.24.461749; this version posted September 25, 2021. The copyright holder for this preprint (which was not certified by peer review) is the author/funder, who has granted bioRxiv a license to display the preprint in perpetuity. It is made available under aCC-BY-NC-ND 4.0 International license.

somatic mutation from whole exome sequencing (WES) of a colorectal tumor specimen from the Yale Cancer Center. Interestingly, T1346I is in the spacer region flanked by BRC2 and BRC3 and is classified as a VUS. Sequence alignment across 9 different species reveal that the S1221 and T1980 residues are highly conserved (**Figure 1B**) whereas T1346 is less well conserved. Multiple studies have verified a conserved core motif within each BRC repeat, designated FxTASGK, that is crucial for RAD51 binding (Bignell *et al.*, 1997; Chen *et al.*, 1998; Lo *et al.*, 2003; Pellegrini *et al.*, 2002). Importantly, both the S1221 and T1980 residues are located directly within this motif (**note the boxed residues in Figure 1B**). Given that structural information is only available for the BRC4 repeat crystallized with the core domain of RAD51 (Pellegrini *et al.*, 2002), we utilized modeling algorithms based on the BRC4 structure to determine if S1221P and T1980I would disrupt key contacts between the BRC2 and BRC7 repeats and RAD51 (**Figure 1C**). The residue T1526 in BRC4 (3rd amino acid position in FxTSAGK) is the equivalent residue to S1221 and T1980 in BRC2 and BRC7, respectively. T1526 is buried in a hydrophobic pocket formed by RAD51 (**Figure 1C, center panel**) (Pellegrini *et al.*, 2002) and the missense mutation, T1526A, has been described to disrupt BRC4 functions (Carreira *et al.*, 2009). Modeling and equivalent predicted amino acid changes were examined closely at T1526 in BRC4 to determine if changes would disrupt the BRC structure or key contacts with RAD51 residues. The T1526A substitution in BRC4 does not lead to steric clashing, however, the electrostatic interactions within the loop are reduced which could disrupt RAD51 binding. Mutating S1221 in the BRC2 model to proline predicts increased steric hindrance of the structure, resulting in a loop to improperly fold to accommodate the bulkier sidechain (**Figure 1C**). Changing T1980 in BRC7 to isoleucine (T1980I) requires a larger sidechain to be incorporated into the structure but with more flexibility than proline. If T1980I is oriented to not misfold, the sidechain is predicted to block RAD51 binding as it would clash with RAD51 residue D187 (**Figure 1C**). Overall, the structural modeling of S1221P and T1980I predicts that either misfolding or steric clashes between residues within the BRC-RAD51

bioRxiv preprint doi: https://doi.org/10.1101/2021.09.24.461749; this version posted September 25, 2021. The copyright holder for this preprint (which was not certified by peer review) is the author/funder, who has granted bioRxiv a license to display the preprint in perpetuity. It is made available under aCC-BY-NC-ND 4.0 International license.

interface could lead to disruption of RAD51 binding. As no structural information exists for the spacer region between BRC2 and BRC3 to date, we were unable to model the T1346I mutation.

S1221P and T1980I variants are defective in response to chemotherapeutics and exhibit diminished ionizing radiation induced RAD51 foci

Although the sequence conservation and homology modeling analysis suggested S1221P and T1980I disrupt RAD51 interactions, we sought to directly test whether the variants in the context of the full-length protein were capable of functionally complementing BRCA2 deficient cells. All full-length BRCA2 cDNA mammalian expression constructs were fused to a tandem repeat of the maltose binding protein tag (2XMBP) which stabilizes and increases BRCA2 expression as previously described (Jensen *et al.*, 2010). We then stably expressed the variants in DLD1 BRCA2$^{-/-}$ cells (Hucl *et al.*, 2008) and successfully derived single cell clones expressing S1221P, T1346I, and T1980I (**Figure 2A**). All cell lines exhibited nuclear localization of BRCA2 by immunofluorescence (**Figure S1A, left panel**) except for null cells as expected. Interestingly, as first described by Baker (Magwood et al., 2013) and confirmed in a subsequent paper by our group (Chatterjee *et al.*, 2016), re-introduction of full-length recombinant protein in BRCA2 deficient cells consistently increases total expression levels of RAD51 (**Figure 2A, Figure S1B**). The basal localization pattern of RAD51 by immunofluorescence also changed from a diffuse cytoplasmic/nuclear staining to a bright distinct signal in the nucleus upon re-expression of WT BRCA2 and the variants in null cells (**Figure S1A**, **middle panel**).

Strikingly, in BRCA2 null cells, neither expression of the S1221P nor the T1980I variant was able to rescue survival to the same level as WT BRCA2 in response to crosslinking agents mitomycin C (MMC) and cisplatin (**Figure 2B**). The two variants did not track with the empty vector control cells suggesting partial complementation was intact in S1221P and T1980I. The survival response of S1221P and T1980I to PARPi (olaparib and talazoparib) was modestly more robust than to crosslinkers but still did not reach the survival capability of WT BRCA2

bioRxiv preprint doi: https://doi.org/10.1101/2021.09.24.461749; this version posted September 25, 2021. The copyright holder for this preprint (which was not certified by peer review) is the author/funder, who has granted bioRxiv a license to display the preprint in perpetuity. It is made available under aCC-BY-NC-ND 4.0 International license.

expressing cells. The T1346I variant provided a full rescue in response to all chemotherapeutic agents tested suggesting this variant was benign (**Figure 2B**). The differential responses of S1221P and T1980I could not be explained by a difference in plating efficiencies (**Figure S2**) nor a dramatic effect upon the percentage change of cells in S phase as measured by EdU incorporation (**Figure S3**). Overall, the results suggest that S1221P and T1980I are hypomorphic alleles of BRCA2.

RAD51 foci formation at sites of DNA DSBs in the nuclei of ionizing radiation damaged cells has long been an established biomarker to indicate functional homologous recombination (Haaf et al., 1995; Rothkamm et al., 2015). In our efforts to provide further insights into the cellular characterization of the three variants, we examined RAD51 foci at 6 hours (peak foci in these cells) after treatment with 12 Gy of ionizing radiation (**Figure 2C).** Phosphorylation of gammaH2AX was used as a surrogate marker for DNA DSBs to ensure the damage inflicted was comparable amongst all cell lines (Chatterjee *et al.*, 2016). The results establish that WT BRCA2 and T1346I can restore RAD51 foci formation in BRCA2 deficient cells, however, the S1221P and T1980I cells displayed an overall significantly lower percentage of cells with foci, again, suggesting a partial defect in HR. Micronuclei formation is an indicator of genomic instability and BRCA2 deficient cells, including the DLD1 BRCA2$^{-/-}$ cells used in this study, contain elevated levels of micronuclei (Ban et al., 2001; Heddle et al., 1983). While WT BRCA2 or T1346I expression in null cells was able to suppress micronuclei formation, T1980I was unable to do so, and S1221P expression appeared to even exacerbate micronuclei formation (see **Figure 2C DAPI panels (right) & quantitation in the lower graph)**.

The purified individual S1221P and T1980I BRC repeats eliminate binding to RAD51

To interrogate whether the binding of the full-length BRCA2 variants to RAD51 was disrupted in the stably complemented cell lines, we utilized amylose pull-down assays to capture BRCA2 and probed for endogenous RAD51 binding by western blotting (**Figure S4A**). Equal levels of RAD51 were pulled down by each BRCA2 variant despite each single BRC

bioRxiv preprint doi: https://doi.org/10.1101/2021.09.24.461749; this version posted September 25, 2021. The copyright holder for this preprint (which was not certified by peer review) is the author/funder, who has granted bioRxiv a license to display the preprint in perpetuity. It is made available under aCC-BY-NC-ND 4.0 International license.

mutation perhaps due to compensatory RAD51 binding by the remaining wild type BRC repeats. We performed the same experiment in a transient transfection approach in 293T cells and observed comparable levels of RAD51 binding across all proteins (**Figure S4B**).

We reasoned that full-length BRCA2 S1221P and T1980I variants appear to bind RAD51 in an equivalent manner to the WT protein either due to the insensitivity of our assay conditions or to the presence of the remaining wild type BRC repeats masking the defect in a single BRC repeat. We explored the first possibility by querying a panel of 2XMBP-BRC repeats consisting of individual as well as multiple BRC repeat fragments: BRC1, 2, 4, 7, BRC1-2, BRC3-4, BRC5-6, BRC7-8, BRC1-4, BRC5-8, and BRC1-8, analyzed as above (**Figure S4A**) to assess their RAD51 binding characteristics (**Figure S5A**). To our surprise, BRC7-8 bound RAD51 while BRC5-6 and the entire BRC5-8 region did not. In a previous study, using the same approach, we had detected a failure of RAD51 to bind to a truncated form of BRCA2 that included both BRC5-8 and the DNA binding domain (DBD), which we had attributed to the DBD portion of the protein (Chatterjee *et al.*, 2016). In contrast, BRC4, BRC1-4, and BRC1-8 fusions with the DBD displayed robust RAD51 binding (Chatterjee *et al.*, 2016). Interestingly, prior yeast two-hybrid analyses had established that all BRC repeats interact with RAD51 except for BRC5 and 6 while a separate study demonstrated that GFP-RAD51 binds GST-BRC7-8 (Wong *et al.*, 1997; Yu et al., 2003). Indeed, we confirmed that BRC7 alone can bind RAD51 under our pull-down conditions (**Figure 3A**, lane 11 and **Figure S5B** lane 15), albeit to a much lesser extent than BRC2 (**Figure 3A**, lane 9).

To circumvent the issue of multiple BRC repeats masking a RAD51 binding defect, we generated a single BRC2 construct incorporating the S1221P variant, and likewise, created a BRC7 construct with the T1980I variant. We included the BRC4 T1526A variant in our analysis, as this variant had previously been described to interfere with RAD51 binding (Tal *et al.*, 2009). The 2XMBP tag alone was used as a negative control in all experiments. By focusing on the individual BRC repeats, both the S1221P and T1980I variants displayed no detectable RAD51

bioRxiv preprint doi: https://doi.org/10.1101/2021.09.24.461749; this version posted September 25, 2021. The copyright holder for this preprint (which was not certified by peer review) is the author/funder, who has granted bioRxiv a license to display the preprint in perpetuity. It is made available under aCC-BY-NC-ND 4.0 International license.

interaction in our pull-down analyses (**Figure 3A,** compare lanes 9 & 10 and lanes 11 & 12 and **Figure S5B**, lanes 16 & 18). As expected by previous reports, T1526A disrupts RAD51 binding (**Figure S5B**, lane 17). To further confirm S1221P and T1980I disrupted RAD51 binding we synthesized the individual peptides (33 amino acids), conjugated them to aminolink resin, and incubated the BRC peptides with purified RAD51. The results clearly demonstrate that wild type BRC2 and BRC7 peptides can interact with RAD51 (**Figure 3B**, lanes 7 & 9) while S1221P and T1980I mutations completely abrogate binding (**Figure 3B**, lanes 8 & 10). Last, incubation of BRC2 peptide with purified RAD51 protein before incubation with overexpressed BRC4 from 293T cells demonstrates that BRC2 binding to RAD51 impede the binding to other BRCs and this phenomenon does not occur with preincubation of S1221P (**Figure S5E**, compare lane 8 and 9).

The BRC repeats are composed of two modules: BRC1-4 mediates binding to free monomeric RAD51 while BRC5-8 binds and stabilizes RAD51-ssDNA complexes (Carreira and Kowalczykowski, 2011). To reconcile our pull-down data demonstrating BRC7 interacts with RAD51 in the absence of filament formation, we considered that RAD51, both in purified form and likely in cell extracts, tends to self-oligomerize which could resemble a filament and mediate the binding activity we observe with both BRC7 and the BRC7-8 peptides. We addressed this discrepancy by interrogating whether the RAD51 T131P mutant was capable of BRC7 interaction. T131P is in the Walker A domain of RAD51, alters ATP binding and hydrolysis behavior preventing filament formation, and acts as a dominant negative when expressed in cells (San Filippo et al., 2006; Wang et al., 2015; Zadorozhny et al., 2017). We confirmed that T131P does not self-associate (**Figure S5D,** lane 8). Indeed, co-incubation of RAD51 T131P with BRC2 exhibited similar binding as wild type RAD51 (**Figure 3C**, compare lanes 2 & 7) whereas binding of T131P to BRC7 was greatly diminished (**Figure 3C,** lane 8). These results reaffirm that BRC2 binds the monomeric form of RAD51 while BRC7 is presumably binding oligomers or self-polymerized forms of RAD51 in our assay. As expected, the S1221P and

bioRxiv preprint doi: https://doi.org/10.1101/2021.09.24.461749; this version posted September 25, 2021. The copyright holder for this preprint (which was not certified by peer review) is the author/funder, who has granted bioRxiv a license to display the preprint in perpetuity. It is made available under aCC-BY-NC-ND 4.0 International license.

T1980I variants failed to bind both wild type RAD51 and the T131P mutant (**Figure 3C,** lanes 4-5 & lanes 9-10).

S1221P and T1980I fail to stimulate RAD51-ssDNA complex formation

To determine whether a lack of RAD51 binding by BRC2-S1221P and BRC7-T1980I alters stimulation/stabilization of a RAD51-ssDNA complex, we utilized an electrophoretic mobility-shift assay (EMSA) under conditions previously described (Carreira and Kowalczykowski, 2011). First, we purified BRC2, BRC7, BRC2-S1221P and BRC7-T1980I from HEK293T cells (**Figure S6A**). We titrated RAD51 protein to determine that 10 nM of RAD51 is the optimal concentration at which RAD51-ssDNA complex formation is approximately 20-30% (Figure **S6B**). Then, RAD51 was incubated with purified BRC2, BRC2-S1221P, BRC7, and BRC7-T1980I proteins followed by the addition of ssDNA (dT40) (**Figure 4A**). As anticipated, increasing concentrations of BRC2 and BRC7 stimulated binding of RAD51 to ssDNA (**Figure 4B,** lanes 3-6, left panel and lanes 3-6, right panel). In contrast, BRC2-S1221P (**Figure 4B**, lanes 7-10, left panel) and BRC7-T1980I (**Figure 4B**, lanes 7-10, right panel) did not stimulate RAD51-ssDNA complex formation even at the highest concentration of BRC proteins (2 μM) tested (**see quantitation in Figure 4C**).

In an orthogonal assay to assess RAD51 filament formation and stabilization, we incubated BRC2, BRC2-S1221P, BRC7, BRC7-T1980I and RAD51 with a 167mer biotinylated ssDNA (**Figure 4D**). The reactions were conducted in the absence of calcium to maintain RAD51 ATPase dependent turnover (Bugreev and Mazin, 2004). The biotin-DNA-RAD51-BRC complexes were then washed extensively, captured on streptavidin magnetic beads, and eluates run on an SDS-PAGE gel. In agreement with the results from our EMSA analyses, BRC2 and BRC7 stabilized RAD51 complex formation on the ssDNA substrate (**Figure 4E**, lanes 5-6 and lanes 11-12) compared to RAD51 alone (**Figure 4E**, lanes 2-3) while BRC2-S1221P (**Figure 4E**, lanes 8-9) and BRC7-T1980I (**Figure 4E**, lanes 14-15) showed little to no increase in bound RAD51. Taken together, the results confirm that the S1221P and T1980I

bioRxiv preprint doi: https://doi.org/10.1101/2021.09.24.461749; this version posted September 25, 2021. The copyright holder for this preprint (which was not certified by peer review) is the author/funder, who has granted bioRxiv a license to display the preprint in perpetuity. It is made available under aCC-BY-NC-ND 4.0 International license.

variants harbor a biochemical defect in the ability to bind and stabilize the RAD51 nucleoprotein complex.

T1980I binds DNA but does not stimulate RAD51-dependent DNA strand exchange

To further probe the impact of the S1221P and T1980I mutations on BRCA2 function, we purified the full-length proteins containing the two variants S1221P and T1980I (**Figure S7A**). Unfortunately, despite extensive troubleshooting, we were unable to purify the full-length S1221P variant protein as it appeared unstable and degraded. Purification of the full-length T1980I protein was successful (**Figure S7A** lane 3). To evaluate the DNA binding profile of purified T1980I, we performed EMSAs on a 3' tail, 5' tail, ssDNA, and dsDNA substrate (**Figure S7C**). T1980I bound all DNA substrates with comparable affinities to WT BRCA2.

We next sought to evaluate whether stimulation of RAD51-mediated DNA strand exchange was impacted by the T1980I variant. We implemented a strategy utilized previously to define the mediator role of wild type BRCA2: (1) we first incubated a 3' tail DNA substrate with RPA, (2) followed by the addition of wild type BRCA2, or T1980I, simultaneously with RAD51, and (3) finally, a radiolabeled donor dsDNA was added to initiate the strand exchange reaction ((Jensen *et al.*, 2010) and **Figure 5A**). Strikingly, T1980I is severely impaired for stimulation of RAD51-mediated DNA strand exchange (**Figure 5B and C**). These results confirm our cell-based findings and define the biochemical defect in T1980I as disruption of RAD51 binding leading to a failure to stimulate RAD51-ssDNA complex formation and subsequent RAD51-mediated DNA strand exchange. Although the full-length BRCA2 S1221P protein proved to be intractable to purification, we speculate that this variant would also fail to stimulate RAD51-mediated DNA strand exchange due to defects in both RAD51 binding and stimulation of RAD51-ssDNA complex formation.

Discussion

The BRCA2 protein mediates a fundamental step in HDR repair of DNA DSBs by binding and delivering multiple RAD51 proteins to resected DNA breaks. By facilitating the

bioRxiv preprint doi: https://doi.org/10.1101/2021.09.24.461749; this version posted September 25, 2021. The copyright holder for this preprint (which was not certified by peer review) is the author/funder, who has granted bioRxiv a license to display the preprint in perpetuity. It is made available under aCC-BY-NC-ND 4.0 International license.

nucleation of RAD51 onto ssDNA, BRCA2 ensures that RAD51 nucleoprotein filament formation can progress leading to strand invasion, homology search, and the eventual exchange of genetic information in the chromosome. Eight BRC repeats, located within proximity to one another, bind RAD51 with varying affinities, and facilitate the loading and nucleation of RAD51 onto ssDNA. Each BRC repeat comprises a highly conserved tetra motif FxTASGK , crucial for BRCA2–RAD51 interactions (**Figure 1A and B**). We took advantage of patient derived missense variants with unknown clinical significance in the BRC repeat region to uncover mechanistic insights into individual BRC function and how these alterations could impact the overall activity of the full-length BRCA2 protein. We found: (1) BRCA2 missense variants S1221P and T1980I, located in a conserved BRC motif (Fx**T**ASGK), disrupt RAD51 binding; (2) the S1221P and T1980I variants are only capable of partial rescue in response to chemotherapeutic agents compared to the wild type protein and a T1346I benign variant; (3) RAD51 foci formation is diminished in cells expressing the S1221P and T1980I variants; (4) the BRC2-S1221P and BRC7-T1980I purified proteins fail to stimulate RAD51-ssDNA complex formation compared to their wild type counterparts; and (5) the full-length purified T1980I BRCA2 protein binds DNA but does not stimulate RAD51-dependent DNA strand exchange. Collectively, our results highlight that single amino acid changes in an individual BRC repeat, within the context of the full-length 3,418 amino acid BRCA2 protein, can have severe consequences on HDR functions.

Our findings that a single amino acid change in BRC2 (S1221P) and BRC7 (T1980I) disrupt RAD51 binding and overall HDR activity emphasize the importance of the serine and threonine residues in the conserved Fx**T**ASGK motif located within each BRC repeat (Lo *et al.*, 2003). Similar defects were reported for the BRC4 mutant T1526A and a BRC3 mutant (Carreira *et al.*, 2009; Davies et al., 2001). The importance of the Fx**T**ASGK motif has been noted in other RAD51 interacting proteins such as RECQL5 and MMS22L. Mutations within the motif that disrupt RAD51 binding downregulate HDR and replication fork protection/stability

bioRxiv preprint doi: https://doi.org/10.1101/2021.09.24.461749; this version posted September 25, 2021. The copyright holder for this preprint (which was not certified by peer review) is the author/funder, who has granted bioRxiv a license to display the preprint in perpetuity. It is made available under aCC-BY-NC-ND 4.0 International license.

activities (Islam et al., 2012; Piwko et al., 2016). Our results further suggest that variants located within the spacer regions between BRC repeats may not affect overall BRCA2 functions, however, more studies are needed with additional variants.

We confirmed that BRC1-2, BRC3-4, BRC7-8 and individual BRC1, 2, 3, 4, 7 and 8 repeats bind RAD51 (**Figure S5A,B**), however, as in our previous findings, BRC5-8 and BRC5-6 do not bind RAD51 in a non-filament form (Chatterjee *et al.*, 2016). Our results agree with prior conclusions from yeast two-hybrid experiments and pull-down interaction studies with GFP-RAD51 in human cells (Wong *et al.*, 1997; Yu *et al.*, 2003). BRC5 and BRC6 are the least conserved repeats potentially explaining the lack of RAD51 binding (Bignell *et al.*, 1997; Lo *et al.*, 2003). We speculate that lack of RAD51 binding through the BRC5-8 module may be due to folding properties that occlude the binding pockets for monomeric RAD51. The lack of binding of BRC7 to RAD51 T131P supports the model that the BRC5-8 module interacts specifically with the RAD51 filament, in agreement with our previous data and prior publications (Carreira and Kowalczykowski, 2011; Chatterjee *et al.*, 2016). Intriguingly, BRC repeats 1-4 can inhibit the ssDNA-dependent ATPase activity of RAD51 whereas BRC repeats 5-8 appear to have no role in this function (Carreira at el PNAS 2011). Conversely, BRC repeats 5-8 stimulate RAD51-ssDNA complex formation through an unknown mechanism and do so to a much greater extent than BRC repeats 1-4 (Carreira at el PNAS 2011). These experiments utilized individual purified BRC repeats, but until our study, no systematic analysis of how each BRC repeat or module contributes to HDR functions within the context of the full-length BRCA2 protein has been performed. Our prior work demonstrated that the BRC5-8 module fused to the DBD of BRCA2 provided a higher level of complementation ability than BRC1-4-DBD, and even surprisingly BRC1-8-DBD, in both cell based and biochemical HDR assays. It remains to be determined why the BRC5-8-DBD protein, which lacks the N-terminus and the BRC1-4 module was more active than other constructs. Future studies using site-directed mutagenesis to inactivate RAD51 binding in individual BRC repeats within the context of the full-length BRCA2

bioRxiv preprint doi: https://doi.org/10.1101/2021.09.24.461749; this version posted September 25, 2021. The copyright holder for this preprint (which was not certified by peer review) is the author/funder, who has granted bioRxiv a license to display the preprint in perpetuity. It is made available under aCC-BY-NC-ND 4.0 International license.

protein, as described here for patient derived missense variants, should clarify the roles of each BRC repeat and how the two modules contribute to HDR functions.

In the past two decades, we have made tremendous progress in delineating the explicit functions of the BRCA2 protein in HDR and fork protection. Nonetheless, the biological significance of multiple RAD51 binding modules located in the center (BRC repeats) and carboxy terminus (S3291) of BRCA2 is still an open question. Furthermore, why does human BRCA2 possess eight BRC repeats whereas other organisms such as *Ustilago maydis* and *Caenorhabditis elegans* contain only one BRC repeat? (Kojic et al., 2002; Martin et al., 2005) The human BRC repeats have been found to interact with RAD51 with varying affinities utilizing methods such as yeast two-hybrid, co-immunoprecipitation, or recombinantly tagged purified proteins (Carreira and Kowalczykowski, 2011; Chatterjee *et al.*, 2016; Chen *et al.*, 1999; Chen *et al.*, 1998; Esashi et al., 2005; Thorslund *et al.*, 2007; Wong *et al.*, 1997) and the emerging theme is that BRC1, 2, 3 and 4 bind monomeric RAD51 with high affinity whereas BRC5, 6, 7, 8 bind weakly. However, BRC5, 6, 7, and 8 significantly stimulate RAD51-ssDNA complex formation implying specific interactions and stabilization of the RAD51 nucleoprotein filament (Carreira and Kowalczykowski, 2011; Chatterjee *et al.*, 2016). While some clarity has been obtained by separating the BRC1-4 and BRC5-8 repeats into distinct functional units, the need for multiple RAD51 interaction sites within BRCA2 remains an enigma. Lastly, the detailed structure and orientation of the eight human BRC repeats within the framework of the full-length BRCA2 protein remains unknown.

Numerous reports in the literature have described tumor-associated missense variants in the BRCA2 protein (Pellegrini *et al.*, 2002; Tal *et al.*, 2009; Venkitaraman, 2002). Our study is the first to provide in-depth evidence of BRCA2 pathogenicity for a biochemical and biological defect of a BRCA2 VUS located in an individual BRC domain. While some studies have functionally demonstrated that BRCA2 hypomorphic mutations exist in the DBD domain (Caburet et al., 2020; Shimelis et al., 2017), comprehensive analyses of BRC domain variants

bioRxiv preprint doi: https://doi.org/10.1101/2021.09.24.461749; this version posted September 25, 2021. The copyright holder for this preprint (which was not certified by peer review) is the author/funder, who has granted bioRxiv a license to display the preprint in perpetuity. It is made available under aCC-BY-NC-ND 4.0 International license.

have been lacking. Our work confirms that site-specific mutations in individual BRC repeats can indeed alter the biochemical HDR functions of BRCA2 leading to cellular defects in response to DNA damage and provides functional evidence for pathogenicity.

Variants described in the literature are often mis-classified as “tumor-associated”, when, they are VUS with unknown impact on protein function, and subsequently, unknown association with tumorigenicity. Classification criteria from online resources such as ClinVar frequently rely on evolutionary sequence conservation or software prediction algorithms, such as SIFT or PolyPhen, to predict pathogenicity rather than functional assays. These uncertainties surrounding interpretation of VUS have become a substantial clinical challenge both for physicians and genetic counselors attempting to take advantage of sequence information to make critical treatment decisions or counsel patients about their future cancer risk. Adoption of functional laboratory-based assays into the clinic has been slow for several reasons including: (1) low throughput, (2) interpretation of results may require substantial HDR and BRCA2 expertise, (3) extensive validation that functional assays correlate with cancer risk, (4) and perhaps skepticism due to a long-standing reliance on familial and genetic linkage data. Nonetheless, considerable progress has been made on several fronts in studying variants located in the DBD domain by examining the HDR functions of BRCA2 using the DR-GFP reporter assay or rescue of mouse embryonic stem cell lethality (Biswas et al., 2011; Biswas et al., 2012; Biswas et al., 2020; Carvalho et al., 2007; Farrugia et al., 2008; Guidugli et al., 2014; Guidugli et al., 2013). Perhaps paradoxically, while BRCA2 pathogenic germline mutations predispose to cancer due to HDR failure and genomic instability, BRCA2 deficient tumors initially respond favorably to platinum drugs and PARPi as opposed to sporadic tumors with BRCA2 functionality intact. Thus, to deliver precision medicine advice to patients, it will be vital to build a comprehensive molecular understanding of variants and how specific defects lead to BRCA2 dysfunction. BRCA2 VUS lack genetic linkage data needed to assess future cancer risk, and thus, functional assays may be the only diagnostic tool available to patients who

bioRxiv preprint doi: https://doi.org/10.1101/2021.09.24.461749; this version posted September 25, 2021. The copyright holder for this preprint (which was not certified by peer review) is the author/funder, who has granted bioRxiv a license to display the preprint in perpetuity. It is made available under aCC-BY-NC-ND 4.0 International license.

harbor rare variants. We propose that rigorous functional assays encompassing orthogonal biochemical and cell-based assays hold promising potential to differentiate pathogenic from benign BRCA2 variants. Finally, patient derived missense variants linked to clinical data will greatly accelerate our understanding of the underlying biology of the BRCA2 protein and the cancer risk associated with mutations in specific domains.

Acknowledgements

We thank Nancy Sanchez for assistance with cloning S1221P mutation and Agata Smogorzewska for the HA RAD51 and HA RAD51 T131P constructs. We thank all members of the Jensen Lab for helpful comments and review of this article.

This research was supported by grants from the NIH (RO1 CA215990), Women's Health Research at Yale, and The Gray Foundation to R.B.J.

bioRxiv preprint doi: https://doi.org/10.1101/2021.09.24.461749; this version posted September 25, 2021. The copyright holder for this preprint (which was not certified by peer review) is the author/funder, who has granted bioRxiv a license to display the preprint in perpetuity. It is made available under aCC-BY-NC-ND 4.0 International license.

Abul-Husn, N.S., Soper, E.R., Odgis, J.A., Cullina, S., Bobo, D., Moscati, A., Rodriguez, J.E., Team, C.G., Regeneron Genetics, C., Loos, R.J.F., et al. (2019). Exome sequencing reveals a high prevalence of BRCA1 and BRCA2 founder variants in a diverse population-based biobank. Genome Med *12*, 2. 10.1186/s13073-019-0691-1.

Anand, R., Pinto, C., and Cejka, P. (2018). Methods to Study DNA End Resection I: Recombinant Protein Purification. Methods Enzymol *600*, 25-66. 10.1016/bs.mie.2017.11.008.

Ban, S., Shinohara, T., Hirai, Y., Moritaku, Y., Cologne, J.B., and MacPhee, D.G. (2001). Chromosomal instability in BRCA1- or BRCA2-defective human cancer cells detected by spontaneous micronucleus assay. Mutat Res *474*, 15-23. 10.1016/s0027-5107(00)00152-4.

Bignell, G., Micklem, G., Stratton, M.R., Ashworth, A., and Wooster, R. (1997). The BRC repeats are conserved in mammalian BRCA2 proteins. Hum Mol Genet *6*, 53-58. 10.1093/hmg/6.1.53.

Biswas, K., Das, R., Alter, B.P., Kuznetsov, S.G., Stauffer, S., North, S.L., Burkett, S., Brody, L.C., Meyer, S., Byrd, R.A., and Sharan, S.K. (2011). A comprehensive functional characterization of BRCA2 variants associated with Fanconi anemia using mouse ES cell-based assay. Blood *118*, 2430-2442. 10.1182/blood-2010-12-324541.

Biswas, K., Das, R., Eggington, J.M., Qiao, H., North, S.L., Stauffer, S., Burkett, S.S., Martin, B.K., Southon, E., Sizemore, S.C., et al. (2012). Functional evaluation of BRCA2 variants mapping to the PALB2-binding and C-terminal DNA-binding domains using a mouse ES cell-based assay. Hum Mol Genet *21*, 3993-4006. 10.1093/hmg/dds222.

Biswas, K., Lipton, G.B., Stauffer, S., Sullivan, T., Cleveland, L., Southon, E., Reid, S., Magidson, V., Iversen, E.S., Jr., and Sharan, S.K. (2020). A computational model for classification of BRCA2 variants using mouse embryonic stem cell-based functional assays. NPJ Genom Med *5*, 52. 10.1038/s41525-020-00158-5.

Bugreev, D.V., and Mazin, A.V. (2004). Ca2+ activates human homologous recombination protein Rad51 by modulating its ATPase activity. Proc Natl Acad Sci U S A *101*, 9988-9993. 10.1073/pnas.0402105101.

Caburet, S., Heddar, A., Dardillac, E., Creux, H., Lambert, M., Messiaen, S., Tourpin, S., Livera, G., Lopez, B.S., and Misrahi, M. (2020). Homozygous hypomorphic BRCA2 variant in primary ovarian insufficiency without cancer or Fanconi anaemia trait. J Med Genet. 10.1136/jmedgenet-2019-106672.

Carreira, A., Hilario, J., Amitani, I., Baskin, R.J., Shivji, M.K., Venkitaraman, A.R., and Kowalczykowski, S.C. (2009). The BRC repeats of BRCA2 modulate the DNA-binding selectivity of RAD51. Cell *136*, 1032-1043. 10.1016/j.cell.2009.02.019.

Carreira, A., and Kowalczykowski, S.C. (2011). Two classes of BRC repeats in BRCA2 promote RAD51 nucleoprotein filament function by distinct mechanisms. Proc Natl Acad Sci U S A *108*, 10448-10453. 10.1073/pnas.1106971108.

Carvalho, M.A., Couch, F.J., and Monteiro, A.N. (2007). Functional assays for BRCA1 and BRCA2. Int J Biochem Cell Biol *39*, 298-310. 10.1016/j.biocel.2006.08.002.

Chatterjee, G., Jimenez-Sainz, J., Presti, T., Nguyen, T., and Jensen, R.B. (2016). Distinct binding of BRCA2 BRC repeats to RAD51 generates differential DNA damage sensitivity. Nucleic Acids Res *44*, 5256-5270. 10.1093/nar/gkw242.

bioRxiv preprint doi: https://doi.org/10.1101/2021.09.24.461749; this version posted September 25, 2021. The copyright holder for this preprint (which was not certified by peer review) is the author/funder, who has granted bioRxiv a license to display the preprint in perpetuity. It is made available under aCC-BY-NC-ND 4.0 International license.

Chen, J.J., Silver, D., Cantor, S., Livingston, D.M., and Scully, R. (1999). BRCA1, BRCA2, and Rad51 operate in a common DNA damage response pathway. Cancer Res *59*, 1752s-1756s.
Chen, P.L., Chen, C.F., Chen, Y., Xiao, J., Sharp, Z.D., and Lee, W.H. (1998). The BRC repeats in BRCA2 are critical for RAD51 binding and resistance to methyl methanesulfonate treatment. Proc Natl Acad Sci U S A *95*, 5287-5292. 10.1073/pnas.95.9.5287.
Consortium, U. (2011). Ongoing and future developments at the Universal Protein Resource. Nucleic Acids Res *39*, D214-D219.
Davies, A.A., Masson, J.Y., McIlwraith, M.J., Stasiak, A.Z., Stasiak, A., Venkitaraman, A.R., and West, S.C. (2001). Role of BRCA2 in control of the RAD51 recombination and DNA repair protein. Mol Cell *7*, 273-282. 10.1016/s1097-2765(01)00175-7.
Esashi, F., Christ, N., Gannon, J., Liu, Y., Hunt, T., Jasin, M., and West, S.C. (2005). CDK-dependent phosphorylation of BRCA2 as a regulatory mechanism for recombinational repair. Nature *434*, 598-604. 10.1038/nature03404.
Esashi, F., Galkin, V.E., Yu, X., Egelman, E.H., and West, S.C. (2007). Stabilization of RAD51 nucleoprotein filaments by the C-terminal region of BRCA2. Nat Struct Mol Biol *14*, 468-474. 10.1038/nsmb1245.
Farrugia, D.J., Agarwal, M.K., Pankratz, V.S., Deffenbaugh, A.M., Pruss, D., Frye, C., Wadum, L., Johnson, K., Mentlick, J., Tavtigian, S.V., et al. (2008). Functional assays for classification of BRCA2 variants of uncertain significance. Cancer Res *68*, 3523-3531. 10.1158/0008-5472.CAN-07-1587.
Guidugli, L., Carreira, A., Caputo, S.M., Ehlen, A., Galli, A., Monteiro, A.N., Neuhausen, S.L., Hansen, T.V., Couch, F.J., Vreeswijk, M.P., and consortium, E. (2014). Functional assays for analysis of variants of uncertain significance in BRCA2. Hum Mutat *35*, 151-164. 10.1002/humu.22478.
Guidugli, L., Pankratz, V.S., Singh, N., Thompson, J., Erding, C.A., Engel, C., Schmutzler, R., Domchek, S., Nathanson, K., Radice, P., et al. (2013). A classification model for BRCA2 DNA binding domain missense variants based on homology-directed repair activity. Cancer Res *73*, 265-275. 10.1158/0008-5472.CAN-12-2081.
Haaf, T., Golub, E.I., Reddy, G., Radding, C.M., and Ward, D.C. (1995). Nuclear foci of mammalian Rad51 recombination protein in somatic cells after DNA damage and its localization in synaptonemal complexes. Proc Natl Acad Sci U S A *92*, 2298-2302. 10.1073/pnas.92.6.2298.
Hall, T.A. (1999). BioEdit: a user-friendly biological sequence alignment editor and analysis program for windows 95/98/NT. In Nucleic acids symposium series *41*, 95-98.
Heddle, J.A., Hite, M., Kirkhart, B., Mavournin, K., MacGregor, J.T., Newell, G.W., and Salamone, M.F. (1983). The induction of micronuclei as a measure of genotoxicity. A report of the U.S. Environmental Protection Agency Gene-Tox Program. Mutat Res *123*, 61-118. 10.1016/0165-1110(83)90047-7.
Hucl, T., Rago, C., Gallmeier, E., Brody, J.R., Gorospe, M., and Kern, S.E. (2008). A syngeneic variance library for functional annotation of human variation: application to BRCA2. Cancer Res *68*, 5023-5030. 10.1158/0008-5472.CAN-07-6189.
Islam, M.N., Paquet, N., Fox, D., 3rd, Dray, E., Zheng, X.F., Klein, H., Sung, P., and Wang, W. (2012). A variant of the breast cancer type 2 susceptibility protein (BRC) repeat is essential for the RECQL5 helicase to interact with RAD51 recombinase for genome stabilization. J Biol Chem *287*, 23808-23818. 10.1074/jbc.M112.375014.

bioRxiv preprint doi: https://doi.org/10.1101/2021.09.24.461749; this version posted September 25, 2021. The copyright holder for this preprint (which was not certified by peer review) is the author/funder, who has granted bioRxiv a license to display the preprint in perpetuity. It is made available under aCC-BY-NC-ND 4.0 International license.

Jensen, R.B., Carreira, A., and Kowalczykowski, S.C. (2010). Purified human BRCA2 stimulates RAD51-mediated recombination. Nature *467*, 678-683. 10.1038/nature09399.
Jimenez-Sainz, J., and Jensen, R.B. (2021). Imprecise Medicine: BRCA2 Variants of Uncertain Significance (VUS), the Challenges and Benefits to Integrate a Functional Assay Workflow with Clinical Decision Rules. Genes (Basel) *12*. 10.3390/genes12050780.
Kojic, M., Kostrub, C.F., Buchman, A.R., and Holloman, W.K. (2002). BRCA2 homolog required for proficiency in DNA repair, recombination, and genome stability in Ustilago maydis. Mol Cell *10*, 683-691. 10.1016/s1097-2765(02)00632-9.
Lahiri, S., and Jensen, R.B. (2021). DNA Strand Exchange to Monitor Human RAD51-Mediated Strand Invasion and Pairing. Methods Mol Biol *2153*, 101-113. 10.1007/978-1-0716-0644-5_8.
Larkin, M.A., Blackshields, G., Brown, N.P., Chenna, R., McGettigan, P.A., McWilliam, H., Valentin, F., Wallace, I.M., Wilm, A., Lopez, R., et al. (2007). Clustal W and Clustal X version 2.0. Bioinformatics *23*, 2947-2948. 10.1093/bioinformatics/btm404.
Liu, J., Doty, T., Gibson, B., and Heyer, W.D. (2010). Human BRCA2 protein promotes RAD51 filament formation on RPA-covered single-stranded DNA. Nat Struct Mol Biol *17*, 1260-1262. 10.1038/nsmb.1904.
Lo, T., Pellegrini, L., Venkitaraman, A.R., and Blundell, T.L. (2003). Sequence fingerprints in BRCA2 and RAD51: implications for DNA repair and cancer. DNA Repair (Amst) *2*, 1015-1028. 10.1016/s1568-7864(03)00097-1.
Magwood, A.C., Malysewich, M.J., Cealic, I., Mundia, M.M., Knapp, J., and Baker, M.D. (2013). Endogenous levels of Rad51 and Brca2 are required for homologous recombination and regulated by homeostatic re-balancing. DNA Repair (Amst) *12*, 1122-1133. 10.1016/j.dnarep.2013.10.006.
Martin, J.S., Winkelmann, N., Petalcorin, M.I., McIlwraith, M.J., and Boulton, S.J. (2005). RAD-51-dependent and -independent roles of a Caenorhabditis elegans BRCA2-related protein during DNA double-strand break repair. Mol Cell Biol *25*, 3127-3139. 10.1128/MCB.25.8.3127-3139.2005.
McAllister, K.A., Haugen-Strano, A., Hagevik, S., Brownlee, H.A., Collins, N.K., Futreal, P.A., Bennett, L.M., and Wiseman, R.W. (1997). Characterization of the rat and mouse homologues of the BRCA2 breast cancer susceptibility gene. Cancer Res *57*, 3121-3125.
Mizuta, R., LaSalle, J.M., Cheng, H.L., Shinohara, A., Ogawa, H., Copeland, N., Jenkins, N.A., Lalande, M., and Alt, F.W. (1997). RAB22 and RAB163/mouse BRCA2: proteins that specifically interact with the RAD51 protein. Proc Natl Acad Sci U S A *94*, 6927-6932. 10.1073/pnas.94.13.6927.
Moynahan, M.E., Pierce, A.J., and Jasin, M. (2001). BRCA2 is required for homology-directed repair of chromosomal breaks. Mol Cell *7*, 263-272. 10.1016/s1097-2765(01)00174-5.
Olopade, O.I., Fackenthal, J.D., Dunston, G., Tainsky, M.A., Collins, F., and Whitfield-Broome, C. (2003). Breast cancer genetics in African Americans. Cancer *97*, 236-245. 10.1002/cncr.11019.
Patel, K.J., Yu, V.P., Lee, H., Corcoran, A., Thistlethwaite, F.C., Evans, M.J., Colledge, W.H., Friedman, L.S., Ponder, B.A., and Venkitaraman, A.R. (1998). Involvement of Brca2 in DNA repair. Mol Cell *1*, 347-357. 10.1016/s1097-2765(00)80035-0.
Pellegrini, L., Yu, D.S., Lo, T., Anand, S., Lee, M., Blundell, T.L., and Venkitaraman, A.R. (2002). Insights into DNA recombination from the structure of a RAD51-BRCA2 complex. Nature *420*, 287-293. 10.1038/nature01230.

bioRxiv preprint doi: https://doi.org/10.1101/2021.09.24.461749; this version posted September 25, 2021. The copyright holder for this preprint (which was not certified by peer review) is the author/funder, who has granted bioRxiv a license to display the preprint in perpetuity. It is made available under aCC-BY-NC-ND 4.0 International license.

Piwko, W., Mlejnkova, L.J., Mutreja, K., Ranjha, L., Stafa, D., Smirnov, A., Brodersen, M.M., Zellweger, R., Sturzenegger, A., Janscak, P., et al. (2016). The MMS22L-TONSL heterodimer directly promotes RAD51-dependent recombination upon replication stress. EMBO J *35*, 2584-2601. 10.15252/embj.201593132.

Rothkamm, K., Barnard, S., Moquet, J., Ellender, M., Rana, Z., and Burdak-Rothkamm, S. (2015). DNA damage foci: Meaning and significance. Environ Mol Mutagen *56*, 491-504. 10.1002/em.21944.

San Filippo, J., Chi, P., Sehorn, M.G., Etchin, J., Krejci, L., and Sung, P. (2006). Recombination mediator and Rad51 targeting activities of a human BRCA2 polypeptide. J Biol Chem *281*, 11649-11657. 10.1074/jbc.M601249200.

Scully, R., and Livingston, D.M. (2000). In search of the tumour-suppressor functions of BRCA1 and BRCA2. Nature *408*, 429-432. 10.1038/35044000.

Sharan, S.K., Morimatsu, M., Albrecht, U., Lim, D.S., Regel, E., Dinh, C., Sands, A., Eichele, G., Hasty, P., and Bradley, A. (1997). Embryonic lethality and radiation hypersensitivity mediated by Rad51 in mice lacking Brca2. Nature *386*, 804-810. 10.1038/386804a0.

Shimelis, H., Mesman, R.L.S., Von Nicolai, C., Ehlen, A., Guidugli, L., Martin, C., Calleja, F., Meeks, H., Hallberg, E., Hinton, J., et al. (2017). BRCA2 Hypomorphic Missense Variants Confer Moderate Risks of Breast Cancer. Cancer Res *77*, 2789-2799. 10.1158/0008-5472.CAN-16-2568.

Spain, B.H., Larson, C.J., Shihabuddin, L.S., Gage, F.H., and Verma, I.M. (1999). Truncated BRCA2 is cytoplasmic: implications for cancer-linked mutations. Proc Natl Acad Sci U S A *96*, 13920-13925. 10.1073/pnas.96.24.13920.

Subramanyam, S., and Spies, M. (2018). Expression, Purification, and Biochemical Evaluation of Human RAD51 Protein. Methods Enzymol *600*, 157-178. 10.1016/bs.mie.2017.11.011.

Tal, A., Arbel-Goren, R., and Stavans, J. (2009). Cancer-associated mutations in BRC domains of BRCA2 affect homologous recombination induced by Rad51. J Mol Biol *393*, 1007-1012. 10.1016/j.jmb.2009.09.011.

Thorslund, T., Esashi, F., and West, S.C. (2007). Interactions between human BRCA2 protein and the meiosis-specific recombinase DMC1. EMBO J *26*, 2915-2922. 10.1038/sj.emboj.7601739.

Venkitaraman, A.R. (2002). Cancer susceptibility and the functions of BRCA1 and BRCA2. Cell *108*, 171-182. 10.1016/s0092-8674(02)00615-3.

Wang, A.T., Kim, T., Wagner, J.E., Conti, B.A., Lach, F.P., Huang, A.L., Molina, H., Sanborn, E.M., Zierhut, H., Cornes, B.K., et al. (2015). A Dominant Mutation in Human RAD51 Reveals Its Function in DNA Interstrand Crosslink Repair Independent of Homologous Recombination. Mol Cell *59*, 478-490. 10.1016/j.molcel.2015.07.009.

Waterhouse, A., Bertoni, M., Bienert, S., Studer, G., Tauriello, G., Gumienny, R., Heer, F.T., de Beer, T.A.P., Rempfer, C., Bordoli, L., et al. (2018). SWISS-MODEL: homology modelling of protein structures and complexes. Nucleic Acids Res *46*, W296-W303. 10.1093/nar/gky427.

Wong, A.K., Pero, R., Ormonde, P.A., Tavtigian, S.V., and Bartel, P.L. (1997). RAD51 interacts with the evolutionarily conserved BRC motifs in the human breast cancer susceptibility gene brca2. J Biol Chem *272*, 31941-31944. 10.1074/jbc.272.51.31941.

Yang, H., Jeffrey, P.D., Miller, J., Kinnucan, E., Sun, Y., Thoma, N.H., Zheng, N., Chen, P.L., Lee, W.H., and Pavletich, N.P. (2002). BRCA2 function in DNA binding and recombination from a BRCA2-DSS1-ssDNA structure. Science *297*, 1837-1848. 10.1126/science.297.5588.1837.

bioRxiv preprint doi: https://doi.org/10.1101/2021.09.24.461749; this version posted September 25, 2021. The copyright holder for this preprint (which was not certified by peer review) is the author/funder, who has granted bioRxiv a license to display the preprint in perpetuity. It is made available under aCC-BY-NC-ND 4.0 International license.

Yu, D.S., Sonoda, E., Takeda, S., Huang, C.L., Pellegrini, L., Blundell, T.L., and Venkitaraman, A.R. (2003). Dynamic control of Rad51 recombinase by self-association and interaction with BRCA2. Mol Cell *12*, 1029-1041. 10.1016/s1097-2765(03)00394-0.

Zadorozhny, K., Sannino, V., Belan, O., Mlcouskova, J., Spirek, M., Costanzo, V., and Krejci, L. (2017). Fanconi-Anemia-Associated Mutations Destabilize RAD51 Filaments and Impair Replication Fork Protection. Cell Rep *21*, 333-340. 10.1016/j.celrep.2017.09.062.

bioRxiv preprint doi: https://doi.org/10.1101/2021.09.24.461749; this version posted September 25, 2021. The copyright holder for this preprint (which was not certified by peer review) is the author/funder, who has granted bioRxiv a license to display the preprint in perpetuity. It is made available under aCC-BY-NC-ND 4.0 International license.

FIGURE LEGENDS

Figure 1. BRCA2 BRC residues S1221, T1346, and T1980 are conserved residues amongst different species. S1221P and T1980I are structurally predicted to disrupt BRC folding and RAD51 binding. (A) BRCA2 protein schematic depicting domain organization: 2XMBP tag, N-terminus, BRC repeats, DNA binding domain (DBD), and C-terminal domain (CTD). BRCA2 missense variants used in this study are indicated with amino acid numbering. **(B)** Multiple Sequence alignment of BRCA2 amino acid sequence from different organisms. Mutated amino acids are indicated in pink and conserved residues are indicated in light grey. BRCA2 amino acid sequences were obtained from Uniprot, and ClustalX (70% threshold for shading) was used for the alignment. Location of the BRCA2 missense variant is displayed: S1221P (BRC2), T1346I (Spacer BRC2-3) and T1980I (BRC7). **(C)** Structural models based on 1N0W structure. Homology model comparison of BRC2 and BRC7 from BRC4. Inset displays BRC4 T1526A. (Below inset) S1221P using BRC2 homology model and T1980I using BRC7 homology model. Alignment of BRC2, BRC4, and BRC7 repeat is displayed. Red box indicates mutated amino acid in the three BRCA2 missense variants.

Figure 2. S1221P and T1980I, but not T1346I, are hypomorphic alleles. T1346I fully rescues DNA damage sensitivity and RAD51 foci formation upon irradiation. (A) Western blot of total cellular lysates from DLD-1 BRCA2$^{-/-}$ cells stably transfected with BRCA2 S1221P (BRC2), T1346I (BRC2-3) and T1980I (BRC7) full-length BRCA2 cDNA constructs. BRCA2 was detected with an MBP antibody. 2XMBP-BRCA2 (470 kDa), and RAD51 (37 kDa). **(B)** Clonogenic survival analyses of stable cell lines expressing BRCA2 Wild Type (WT), S1221P, T1346I, and T1980I variants upon treatment with mitomycin C or cisplatin for 1 hour or Olaparib or Talazoparib for 24 hours. **(C)** Immunofluorescence images and quantification of RAD51 (green) and gammaH2AX (red) foci, and DAPI staining to visualize nuclei (blue, grey) and micronuclei (grey). Representative images at 6 hr post-IR 12 Gy. Quantification of 4 independent experiments and statistical analysis t-test and one-way ANOVA. Scale bar represents 50 µm. *p value<0.05 ****p value<0.0001.

Figure 3. BRC2-S1221P and BRC7-T1980I disrupt RAD51 binding. (A) Schematic of amylose pull-down reaction to detect RAD51 binding. **(B)** Total cellular lysates (TCL) and amylose pull-downs from HEK 293T cells transiently transfected with 2XMBP, 2XMBP-BRC2, 2XMBP-BRC2 S1221P, 2XMBP-BRC7, and 2XMBP-BRC7 T1980I. Western blot: anti-MBP was used to detect 2XMBP-BRC and anti-RAD51 to detect endogenous RAD51. **(C)** Schematic of aminolink-conjugated resin reaction to BRC peptides and pull-down reaction to detect in vitro RAD51 binding. **(D)** Synthesized peptides (BRC2, BRC2 S1221P, BRC7, BRC7 T1980I) (35 amino acids length) were conjugated to aminolink resin and incubated with purified RAD51. Western blot using RAD51 antibody to detect unbound and bound RAD51 after washing and elution of proteins off resin in laemmli sample buffer. **(E)** Total cellular lysates (TCL) and amylose pull-downs of HEK 293T cells transiently transfected with 2XMBP, 2XMBP-BRC2, 2XMBP-BRC2-S1221P, 2XMBP BRC7, 2XMBP-BRC7 T1980I, HA-RAD51 wild type and HA-RAD51 T131P. Anti-MBP was used to detect 2XMBP-BRC. HA antibody was used to detect recombinant RAD51.

Figure 4. BRC2-S1221P and BRC7-T1980I fail to stimulate RAD51-ssDNA complex formation. (A) Schematic of reaction to assay BRC repeat stimulation of RAD51-ssDNA complex formation by EMSA. RAD51 was pre-incubated with increasing amounts of BRC protein for 15 minutes then radiolabeled ssDNA (dT40) was added for 40 minutes. All reactions

bioRxiv preprint doi: https://doi.org/10.1101/2021.09.24.461749; this version posted September 25, 2021. The copyright holder for this preprint (which was not certified by peer review) is the author/funder, who has granted bioRxiv a license to display the preprint in perpetuity. It is made available under aCC-BY-NC-ND 4.0 International license.

were incubated at 37 degrees and visualized on a 6% TAE polyacrylamide gel. **(B)** Autoradiograms of EMSA gels depicting increasing concentration of BRC proteins: BRC2, BRC2-S1221P, BRC7, BRC7-T1980I incubated with 10 nM RAD51, and 400 pM ssDNA (Oligo dT40*) Gel represents no protein (lane 1), RAD51 (lane 2), BRC2 or BRC7 (lane 3-6) and BRC2-S1221P or BRC7-T1980I (lane 7-10). **(C)** Quantification of BRC-RAD51-ssDNA complexes in the presence of increasing concentrations of BRC2, BRC2-S1221P, BRC7, BRC7-T1980I calculated from gels shown in B. Error bars represent the S.D. for two independent experiments. **(D)** Schematic of biotinylated DNA pull-down assay. Purified BRC proteins were pre-incubated with increasing concentrations of purified RAD51 for 10 min. Biotinylated ssDNA (167-mer) was then added for 10 minutes to allow nucleoprotein filament formation and captured on magnetic streptavidin beads. The beads were then washed, eluted in sample buffer, and analyzed by SDS-PAGE and western blotting **(E)** Western blot depicting amount of RAD51 pulled down and eluted from biotin-DNA-BRC-RAD51 complexes. RAD51 concentrations from 0-100 nM were pre-incubated with 80 nM of BRC peptide, incubated with biotin-ssDNA, washed extensively, and then eluted. Gel represents RAD51 alone (lane 1-3), RAD51+BRC2 (lane 4-6), RAD51+BRC2-S1221P (lane 7-9), RAD51+BRC7 (lane 10-12), RAD51+BRC7-T1980I (lane 13-15).

Figure 5. RAD51-mediated DNA strand exchange activity is stimulated by increasing amounts of WT BRCA2 but not T1980I. (A) Diagram of DNA strand exchange assay. RPA was pre-bound to the 3' tail DNA substrate for 5 minutes. Increasing amounts of WT BRCA2 or T1980I protein was then added in combination with RAD51 for 5 minutes, followed by the addition of radiolabeled donor dsDNA for 30 minutes. All reactions were incubated at 37 degrees. The reaction was then deproteinized and run on a 6% TAE polyacrylamide gel. **(B)** Autoradiograms of PAGE gels used to analyze the products of DNA strand exchange. The first lane is a no protein control. The second lane contains RAD51 in the absence of RPA or BRCA2. **(C)** Quantification of the product formation and mean values from three independent experiments were plotted. Errors bars represent the S.D. of three independent experiments.

bioRxiv preprint doi: https://doi.org/10.1101/2021.09.24.461749; this version posted September 25, 2021. The copyright holder for this preprint (which was not certified by peer review) is the author/funder, who has granted bioRxiv a license to display the preprint in perpetuity. It is made available under aCC-BY-NC-ND 4.0 International license.

SUPPLEMENTARY FIGURES

Supplementary Figure 1: S1221P, T1346I, and T1980I full-length BRCA2 proteins localize to the nucleus. Localization by immunofluorescence of untreated BRCA2$^{-/-}$, BRCA2 WT, S1221P, T1346I, and T1980I stable cell lines. Representative images of 2XMBP-BRCA2 (red, anti-MBP), RAD51 (green), and nuclei (blue).

Supplementary Figure 2: BRCA2$^{-/-}$ cells stably expressing full-length 2XMBP-BRCA2 S1221P and T1980I only partially rescue sensitivity to crosslinking agents (MMC or cisplatin) and PARP inhibitors (Olaparib or Talazoparib). 2XMBP-BRCA2 WT and T1346I protein expression rescue to the same extent upon exposure to crosslinking agents and PARP inhibitors. Representative images of cell colonies stained with crystal violet 14 days after treatment. PE; plating efficiency. Treatments: 2.5 µM MMC 1hr, 25 µM Cisplatin 1hr, 15 µM Olaparib 24 hr, 20 nM Talazoparib 24 hr.

Supplementary Figure 3: Expression of S1221P, T1346I, or T1980I in BRCA2 deficient cells with or without DNA damage does not affect percentage of cells in S phase. Quantification of EdU positive cells for 5 hr post IR 12 Gy or 5 hr with the treatments 10 µM MMC or 50 µM Olaparib. Data from 3 independent experiments. *p value<0.05

Supplementary Figure 4: S1221P, T1346I, and T1980I full-length BRCA2 proteins bind RAD51. (A) Western blots of total cell lysates (TCL) (left gel) or amylose pull-downs (right gel) from stable cell lines expressing full-length BRCA2 WT, S1221P, T1346I, and T1980I. 2XMBP-BRCA2 (470 kDa) detected using a C-terminal antibody. Depicted RAD51 is endogenous (37 kDa). **(B)** Western blot of total cellular lysates (TCL) and amylose pull-downs from HEK 293T cells transiently transfected with 2XMBP-BRCA2 WT, S1221P, T1346I, and T1980I full-length constructs. Anti-MBP antibody was used for BRCA2 detection. Lower red arrow in the Stain Free panel indicates 2XMBP and upper red arrow indicates 2XMBP BRCA2 expression. Graphs on the right represent RAD51 quantification from the western blot of total cellular lysates

Supplementary Figure 5. BRC1-2, BRC7-8, BRC2, and BRC7 bind RAD51 whereas BRC2-S1221P and BRC7-T1980I disrupt RAD51 binding. (A) Western blot of total cellular lysates (TCL) and amylose pull-downs from HEK 293T cells transiently transfected with 2XMBP or 2XMBP-BRC repeat constructs: BRC1-8, BRC1-4, BRC5-8, BRC1-2, BRC3-4, BRC 5-6 and BRC 7-8. **(B)** Western blot of total cellular lysates (TCL) and amylose pull-downs from HEK 293T cells transiently transfected with 2XMBP or 2XMBP BRC constructs: BRC1, BRC2, BRC4, BRC7, BRC2-S1221P, BRC4-T1526A and BRC7-T1980I. BRC constructs were detected with an MBP antibody **(C)** Pull-downs with synthetic peptides: BRC2, BRC2-S1221P, BRC7, BRC7-T1980I fused to aminolink resin. 10 µL of aminolink resin conjugated to each peptide was incubated with increasing concentrations of purified RAD51 protein. Western blot (anti-RAD51) from unbound (UB) and bound (B) elutions from aminolink resin. **(D)** Western blot of total cellular lysates and amylose pulldowns from HEK 293T cells transiently transfected with 2XMBP, 2XMBP-RAD51, HA-RAD51, HA-RAD51 T131P. RAD51 was detected with an HA antibody. **(E)** Western blots from peptide competition assay. Purified RAD51 previously incubated with or without BRC2 or BRC2-S1221P peptide was utilized in an amylose pull-down assay with 2XMBP-BRC4 or 2XMBP-BRC4-T1526A recombinantly expressed in HEK 293T cells. BRC repeat proteins detected with anti-MBP. Purified RAD51 eluted from amylose beads bound to 2XMBP-BRC peptide detected with anti-RAD51.

bioRxiv preprint doi: https://doi.org/10.1101/2021.09.24.461749; this version posted September 25, 2021. The copyright holder for this preprint (which was not certified by peer review) is the author/funder, who has granted bioRxiv a license to display the preprint in perpetuity. It is made available under aCC-BY-NC-ND 4.0 International license.

Supplementary Figure 6. Purification of 2XMBP-BRC fragments from human 293T cells. RAD51 and RPA purified from E. Coli. Optimization of RAD51-ssDNA EMSA (A) Coomassie stained gel of BRC2, BRC2-S1221P, BRC7 and BRC7-T1980I proteins purified from HEK 293T cells and RAD51 and RPA proteins purified from bacteria used for biochemical experiments. **(B)** Increasing concentrations of purified RAD51 were incubated with radiolabeled dT40 and analyzed by EMSA.

Supplementary Figure 7. Full-length BRCA2 WT and T1980I purified proteins bind various DNA substrates with similar efficiencies. (A) Stain Free gel of 2XMBP-BRCA2 full-length purified proteins from 293T cells. The 450 mM NaCl elution fractions from a HiTrap Q column were run on a 4-15% gradient SDS-PAGE gel. **(B)** Autoradiograms of DNA strand exchange assays. The first lane is a no protein control. The second lane contains RAD51 in the absence of RPA or BRCA2. Lanes 3-6 contain increasing concentrations of RPA first. Lanes 7-9 depict increasing concentrations of BRCA2 overcome RPA blockade of RAD51-mediated DNA strand exchange. **(C)** EMSAs depicting increasing concentrations of BRCA2 WT and T1980I proteins incubated with 3' tail, 5' tail, ssDNA, and dsDNA substrates. Percentage of protein-DNA complex was calculated as the free DNA remaining in a lane relative to the protein-free lane (0% complex or 100% free DNA). Error bars are S.D. from 3 independent experiments.

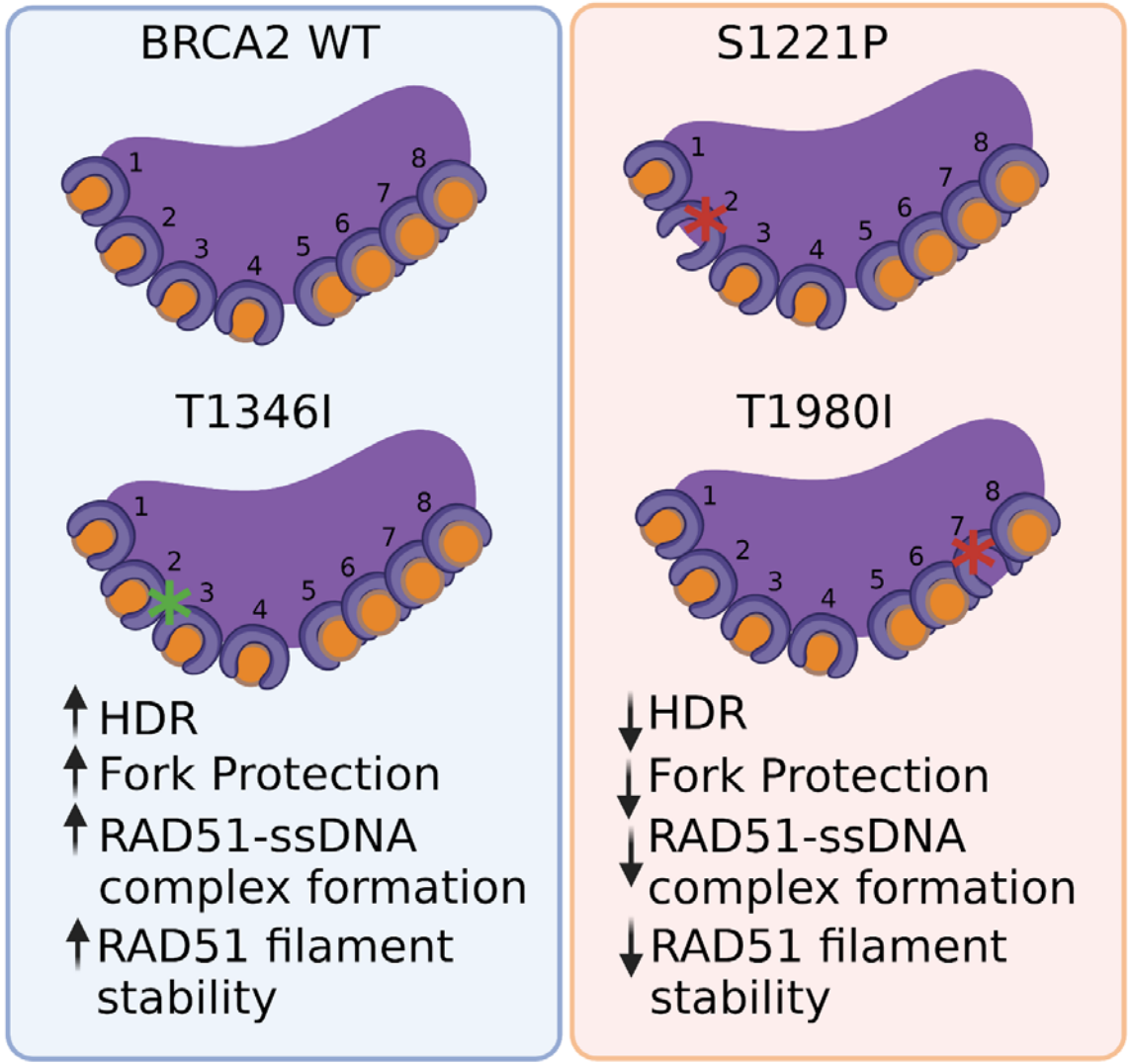

Graphical Abstract

bioRxiv preprint doi: https://doi.org/10.1101/2021.09.24.461749; this version posted September 25, 2021. The copyright holder for this preprint (which was not certified by peer review) is the author/funder, who has granted bioRxiv a license to display the preprint in perpetuity. It is made available under aCC-BY-NC-ND 4.0 International license.

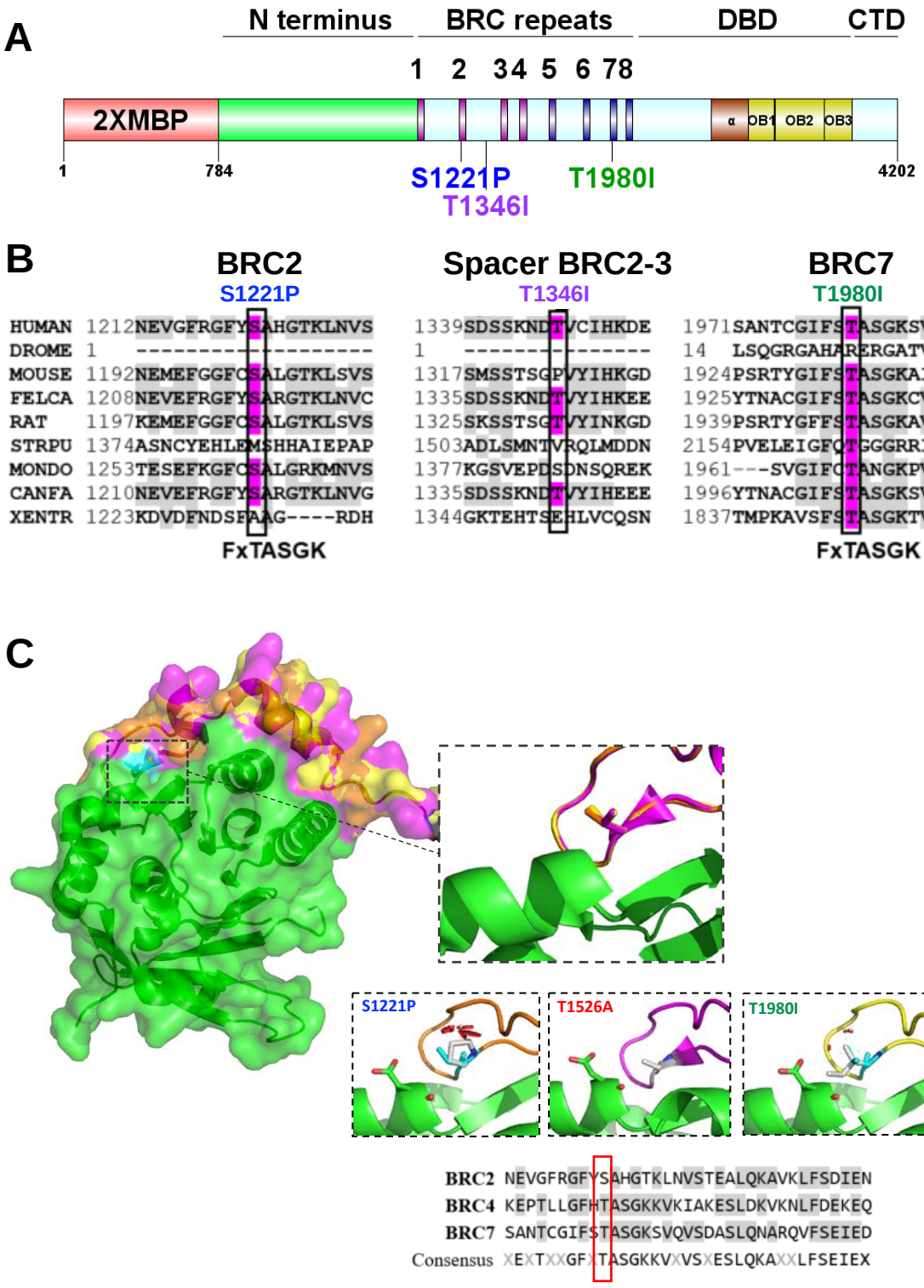

Figure 1

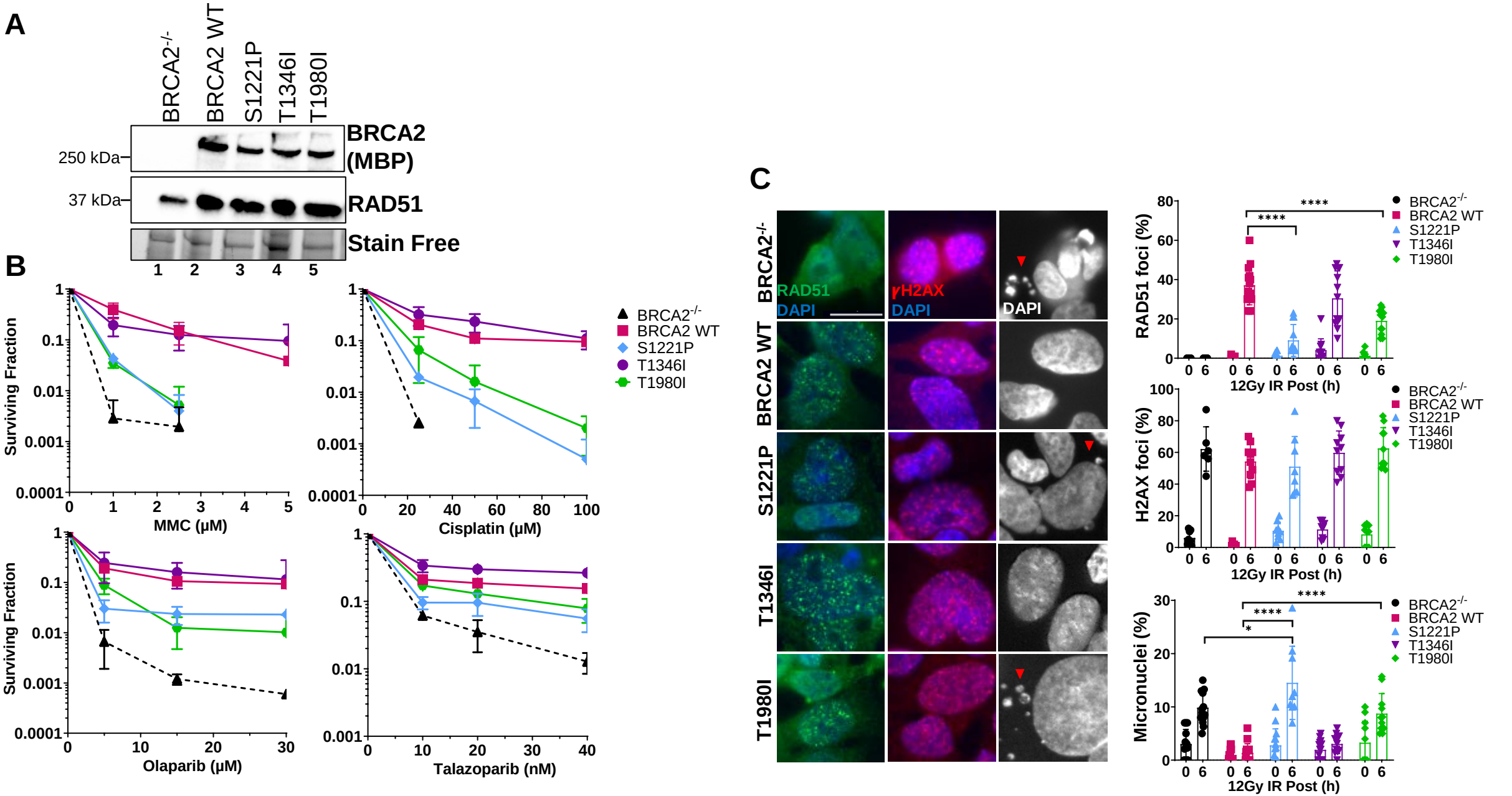
A
BRCA2-/-
BRCA2 WT
S1221P
T1346I
T1980I
250 kDa
BRCA2 (MBP)
37 kDa
RAD51
Stain Free
1 2 3 4 5
B
Surviving Fraction
MMC (μM)
Cisplatin (μM)
Olaparib (μM)
Talazoparib (nM)
BRCA2-/-
BRCA2 WT
S1221P
T1346I
T1980I
C
BRCA2-/-
BRCA2 WT
S1221P
T1346I
T1980I
RAD51
DAPI
γH2AX
DAPI
DAPI
RAD51 foci (%)
H2AX foci (%)
Micronuclei (%)
12Gy IR Post (h)
****
*

Figure 2

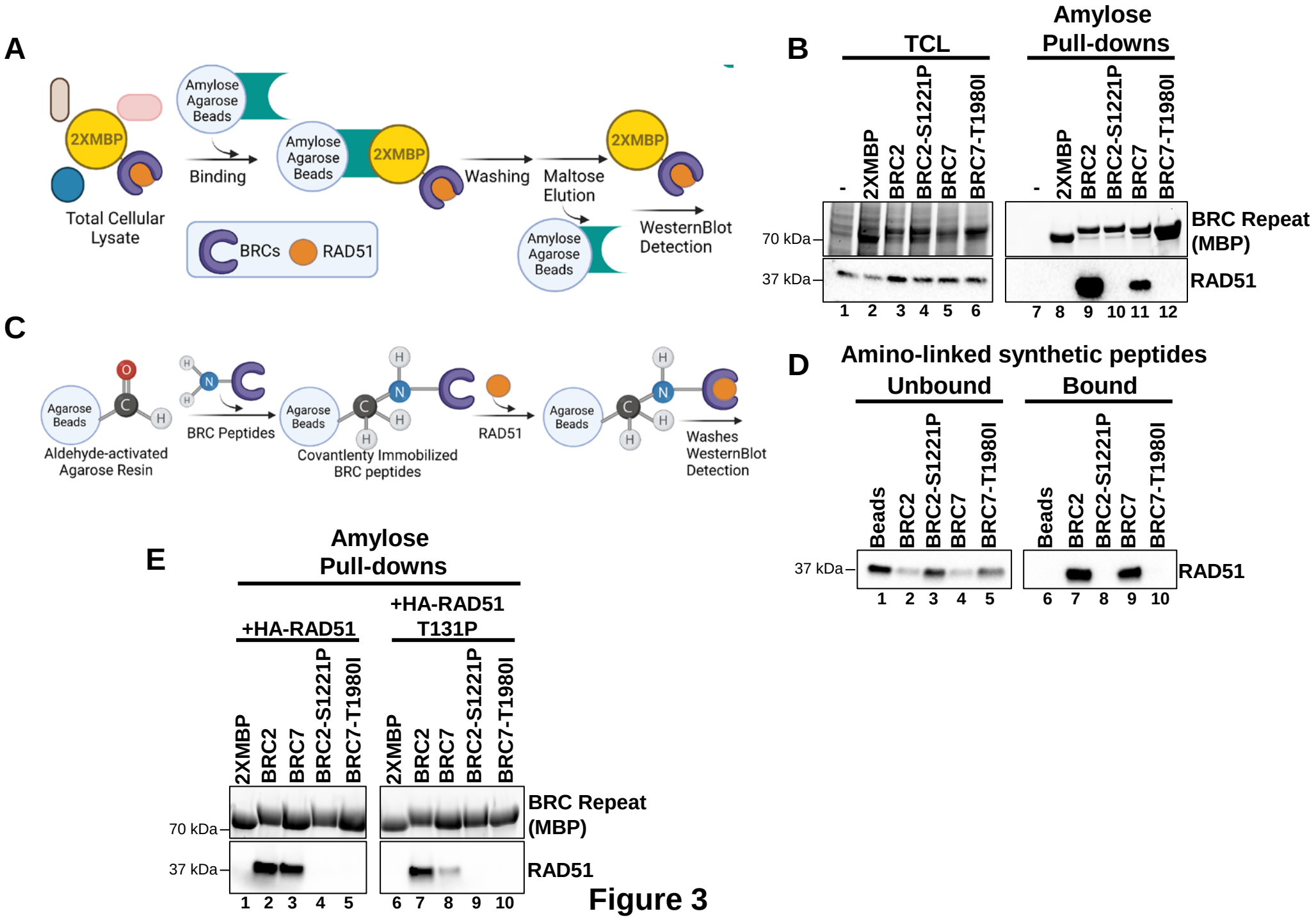
A
Amylose Agarose Beads
2XMBP
Binding
Amylose Agarose Beads
2XMBP
Washing
Maltose Elution
2XMBP
Total Cellular Lysate
BRCs
RAD51
Amylose Agarose Beads
WesternBlot Detection
B
TCL
Amylose Pull-downs
-
2XMBP
BRC2
BRC2-S1221P
BRC7
BRC7-T1980I
70 kDa
37 kDa
BRC Repeat (MBP)
RAD51
1 2 3 4 5 6
7 8 9 10 11 12
C
Agarose Beads
Aldehyde-activated Agarose Resin
BRC Peptides
Agarose Beads
Covantlenty Immobilized BRC peptides
RAD51
Agarose Beads
Washes WesternBlot Detection
D
Amino-linked synthetic peptides
Unbound
Bound
Beads
BRC2
BRC2-S1221P
BRC7
BRC7-T1980I
37 kDa
RAD51
1 2 3 4 5
6 7 8 9 10
E
Amylose Pull-downs
+HA-RAD51
+HA-RAD51 T131P
2XMBP
BRC2
BRC7
BRC2-S1221P
BRC7-T1980I
70 kDa
37 kDa
BRC Repeat (MBP)
RAD51
1 2 3 4 5
6 7 8 9 10

Figure 3

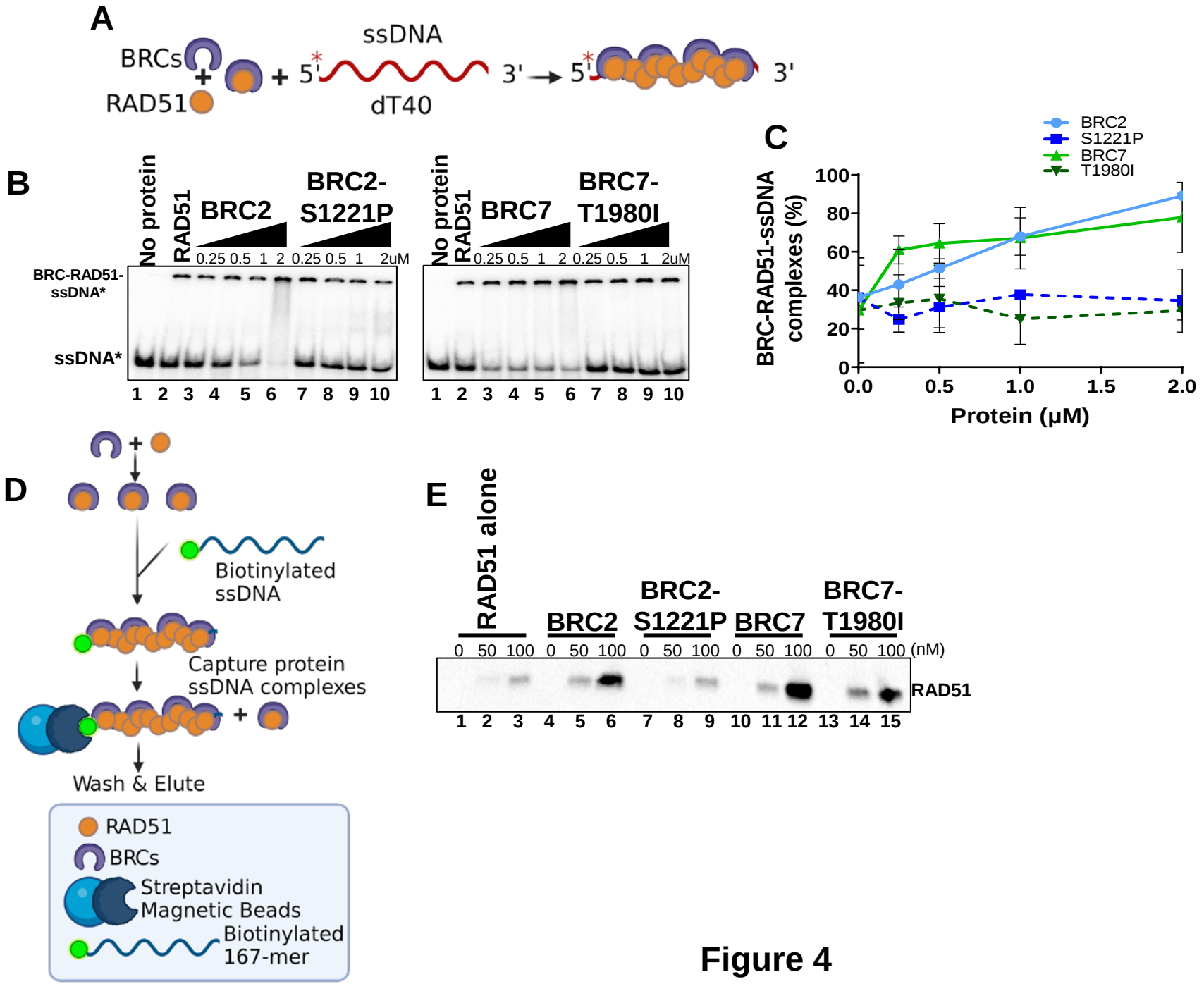
A
BRCs
RAD51
ssDNA
5'
dT40
3'
5'
3'
B
No protein
RAD51
BRC2
BRC2-S1221P
0.25 0.5 1 2 0.25 0.5 1 2uM
BRC-RAD51-ssDNA*
ssDNA*
1 2 3 4 5 6 7 8 9 10
No protein
RAD51
BRC7
BRC7-T1980I
0.25 0.5 1 2 0.25 0.5 1 2uM
1 2 3 4 5 6 7 8 9 10
C
BRC2
S1221P
BRC7
T1980I
BRC-RAD51-ssDNA complexes (%)
100
80
60
40
20
0
0.0 0.5 1.0 1.5 2.0
Protein (μM)
D
Biotinylated ssDNA
Capture protein ssDNA complexes
Wash & Elute
RAD51
BRCs
Streptavidin Magnetic Beads
Biotinylated 167-mer
E
RAD51 alone
BRC2
BRC2-S1221P
BRC7
BRC7-T1980I
0 50 100 0 50 100 0 50 100 0 50 100 0 50 100 (nM)
RAD51
1 2 3 4 5 6 7 8 9 10 11 12 13 14 15

Figure 4

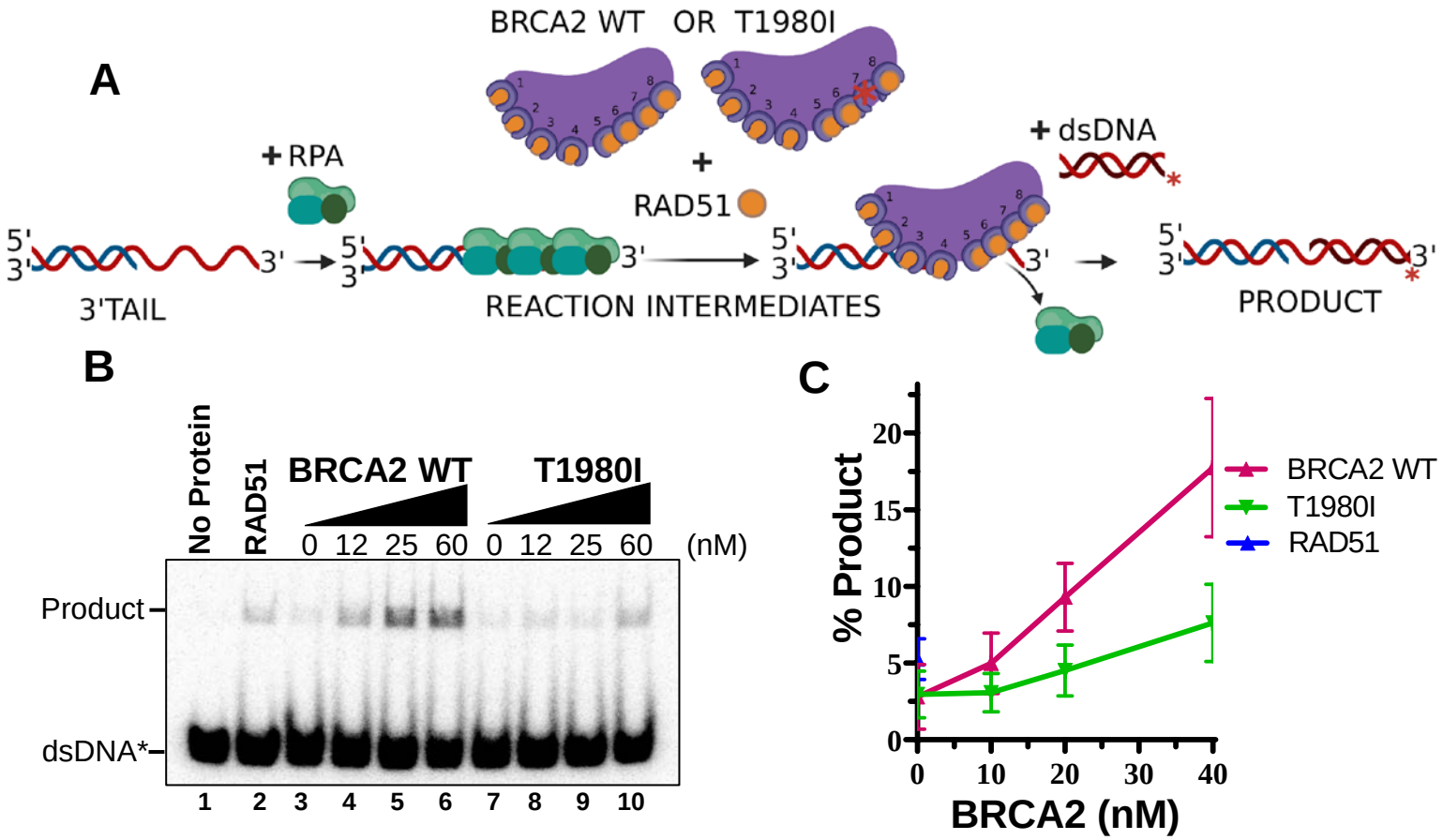

Created with BioRender.com

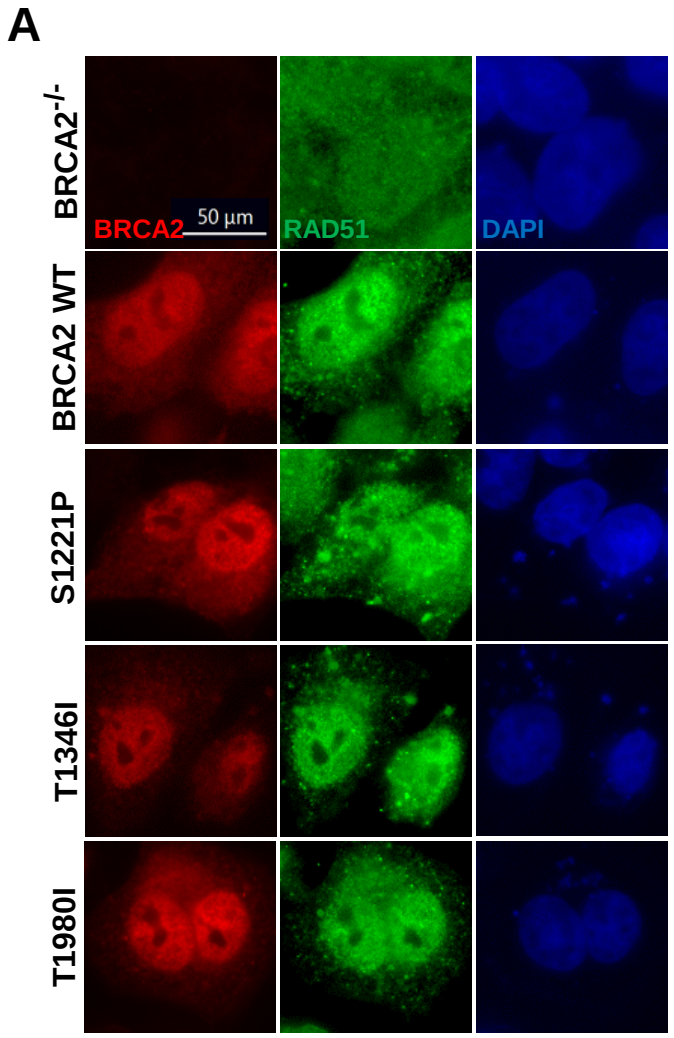

Supplementary Figure 1

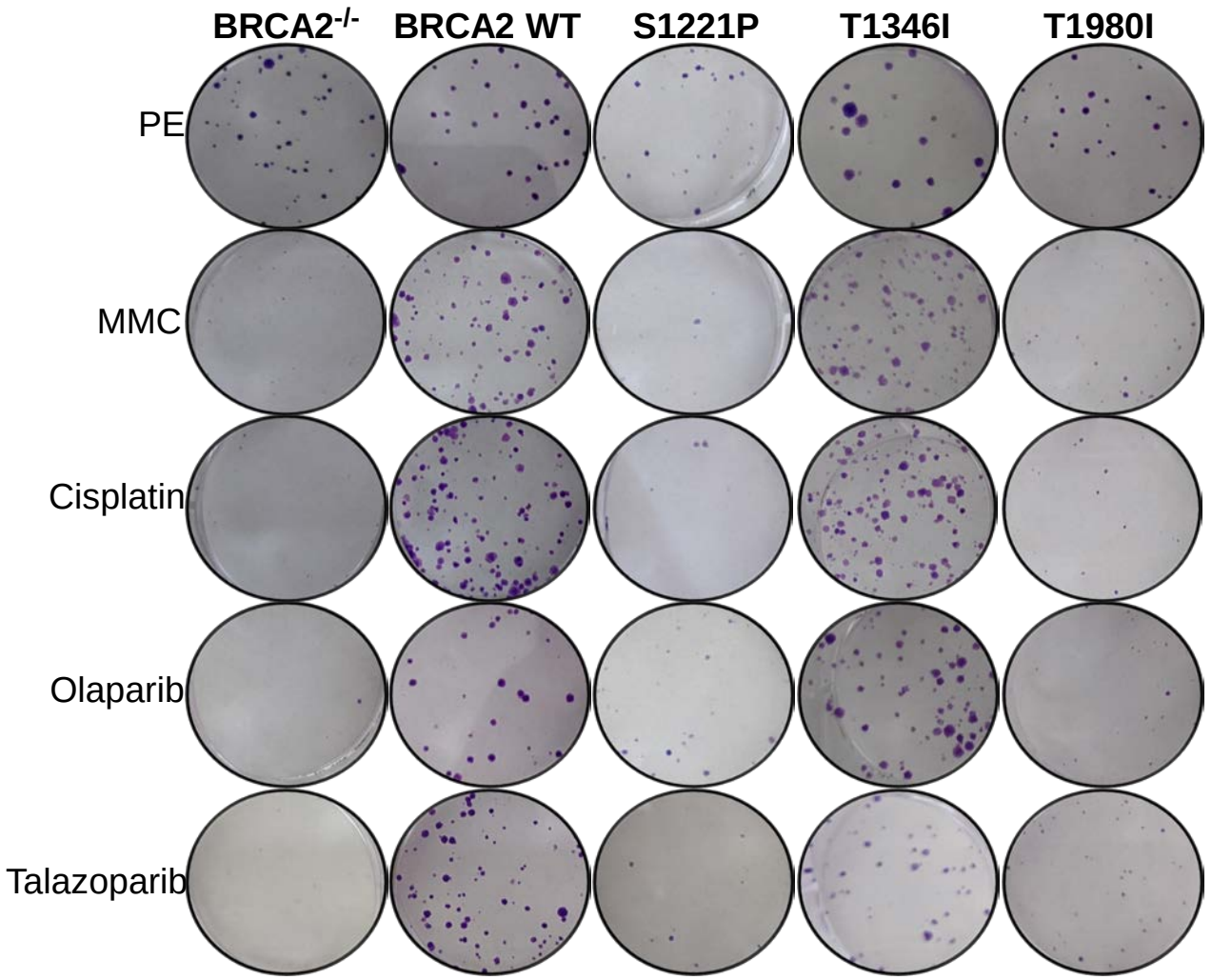

Supplementary Figure 2

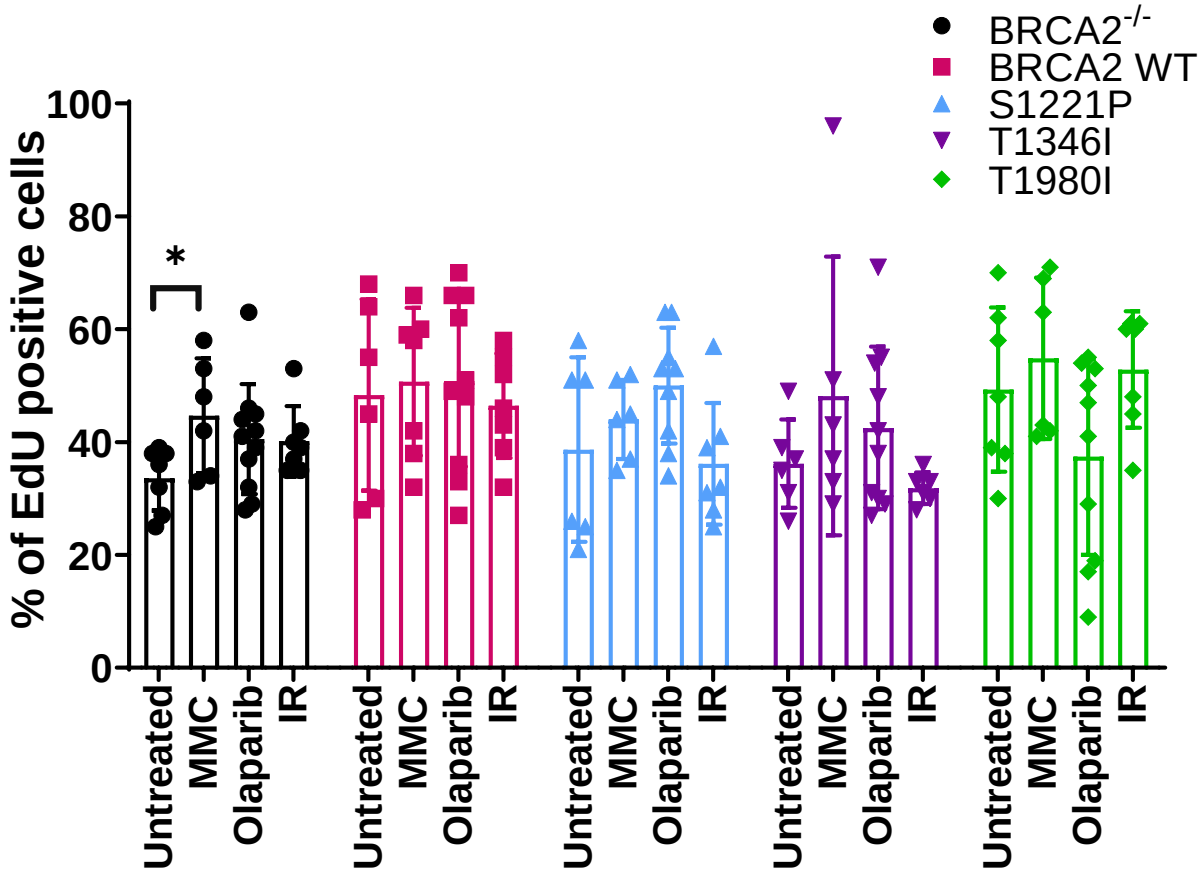

Supplementary Figure 3

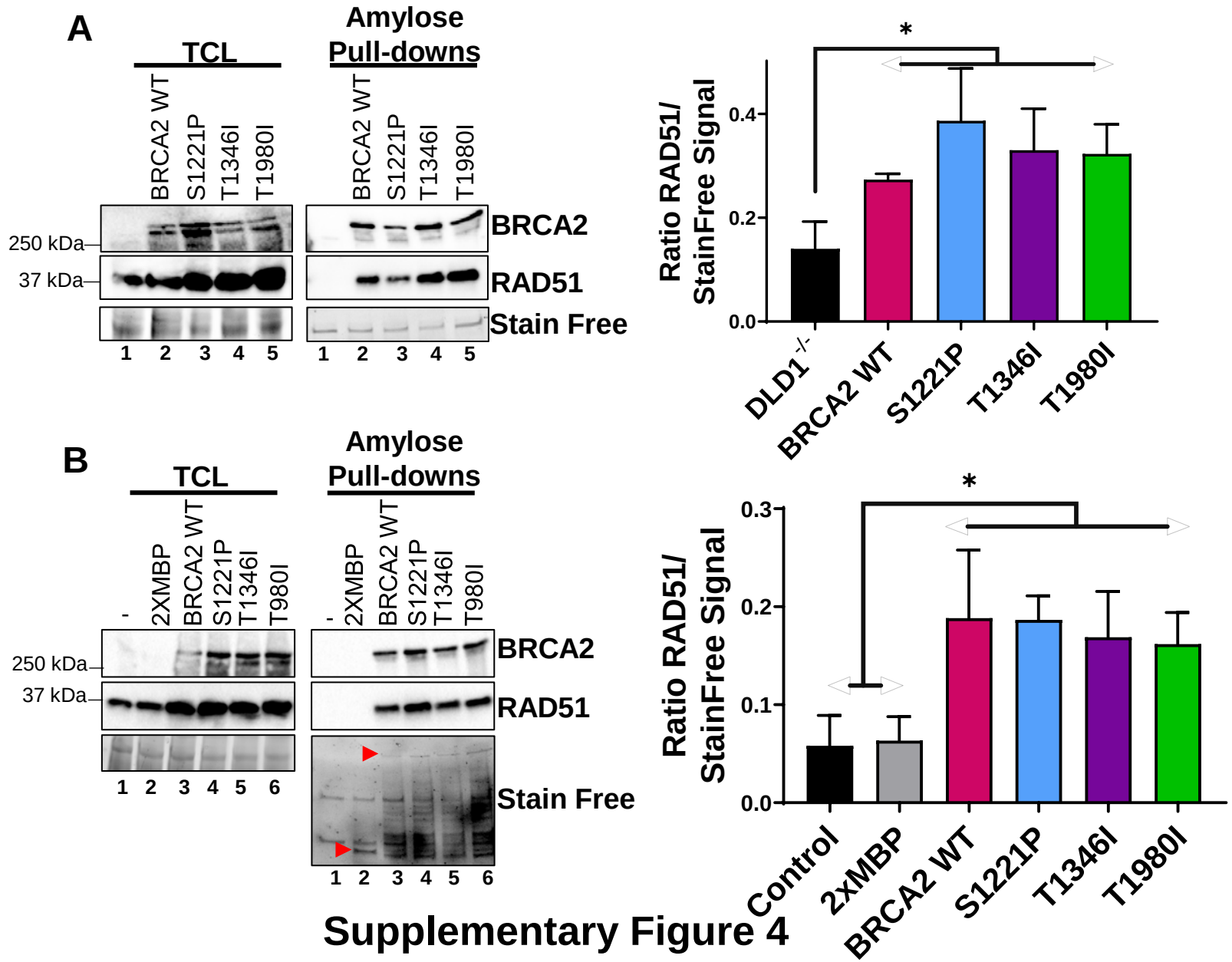

Supplementary Figure 4

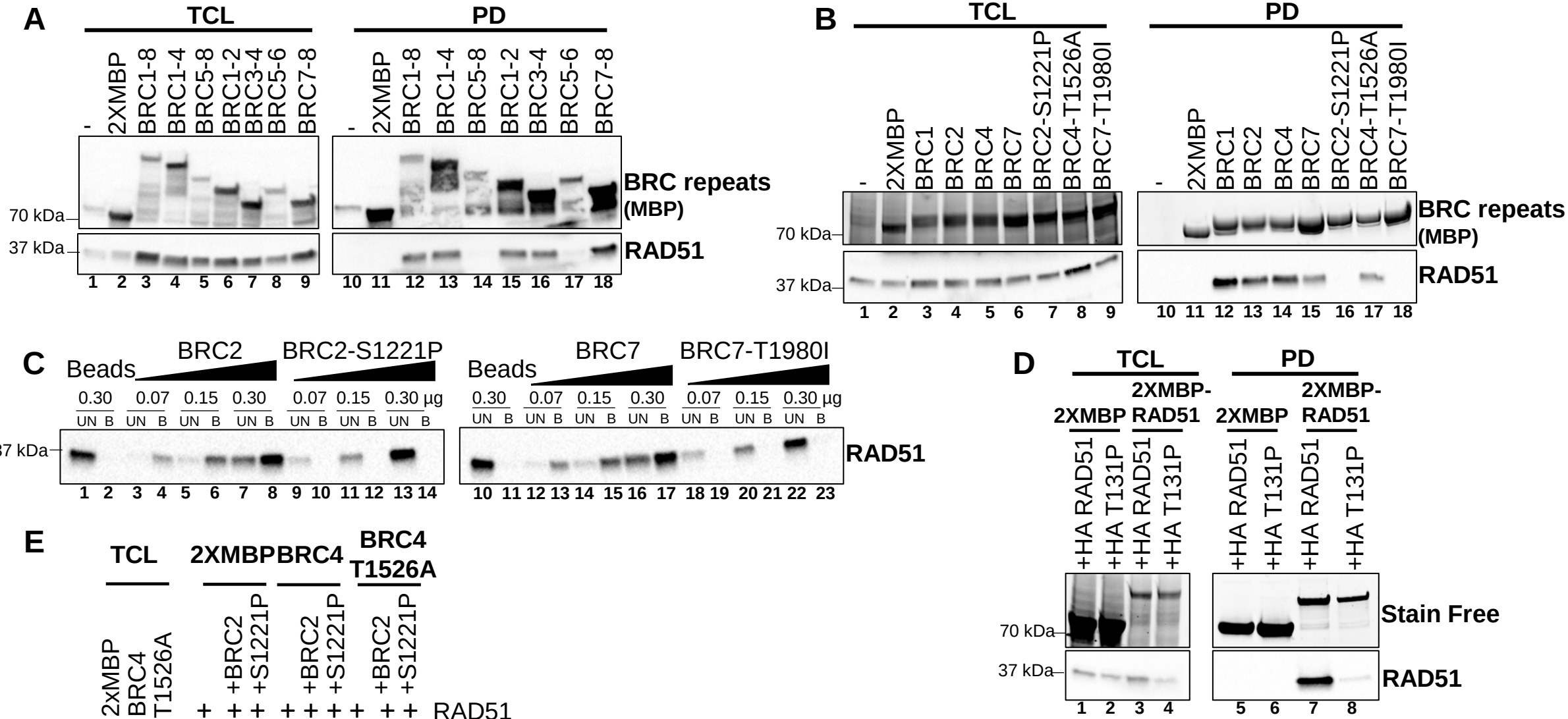

Supplementary Figure 5

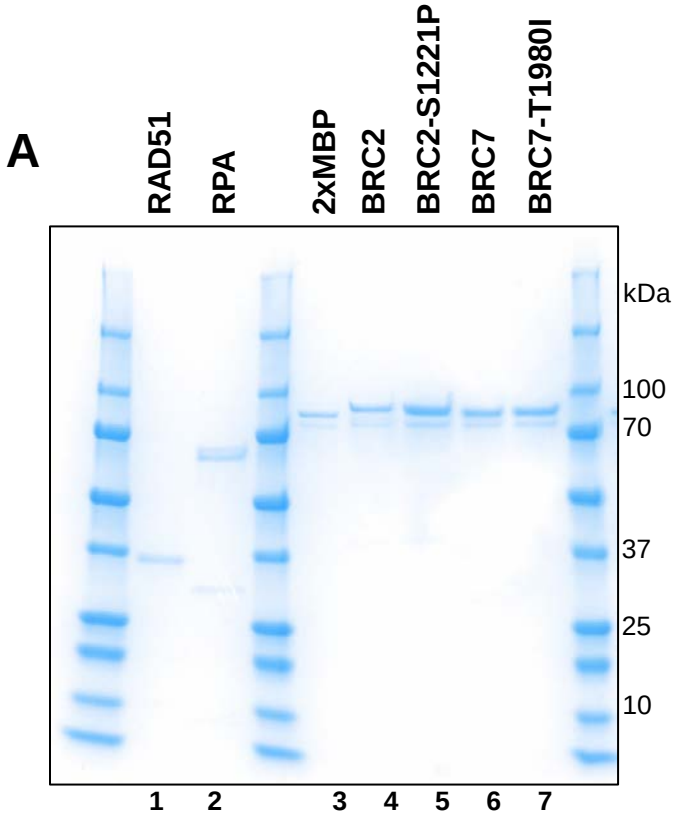

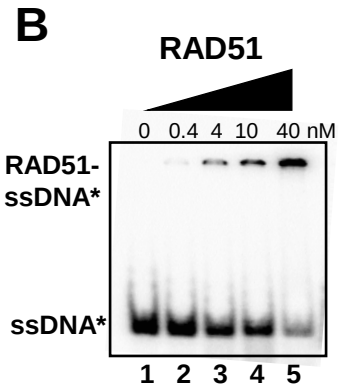

Supplementary Figure 6

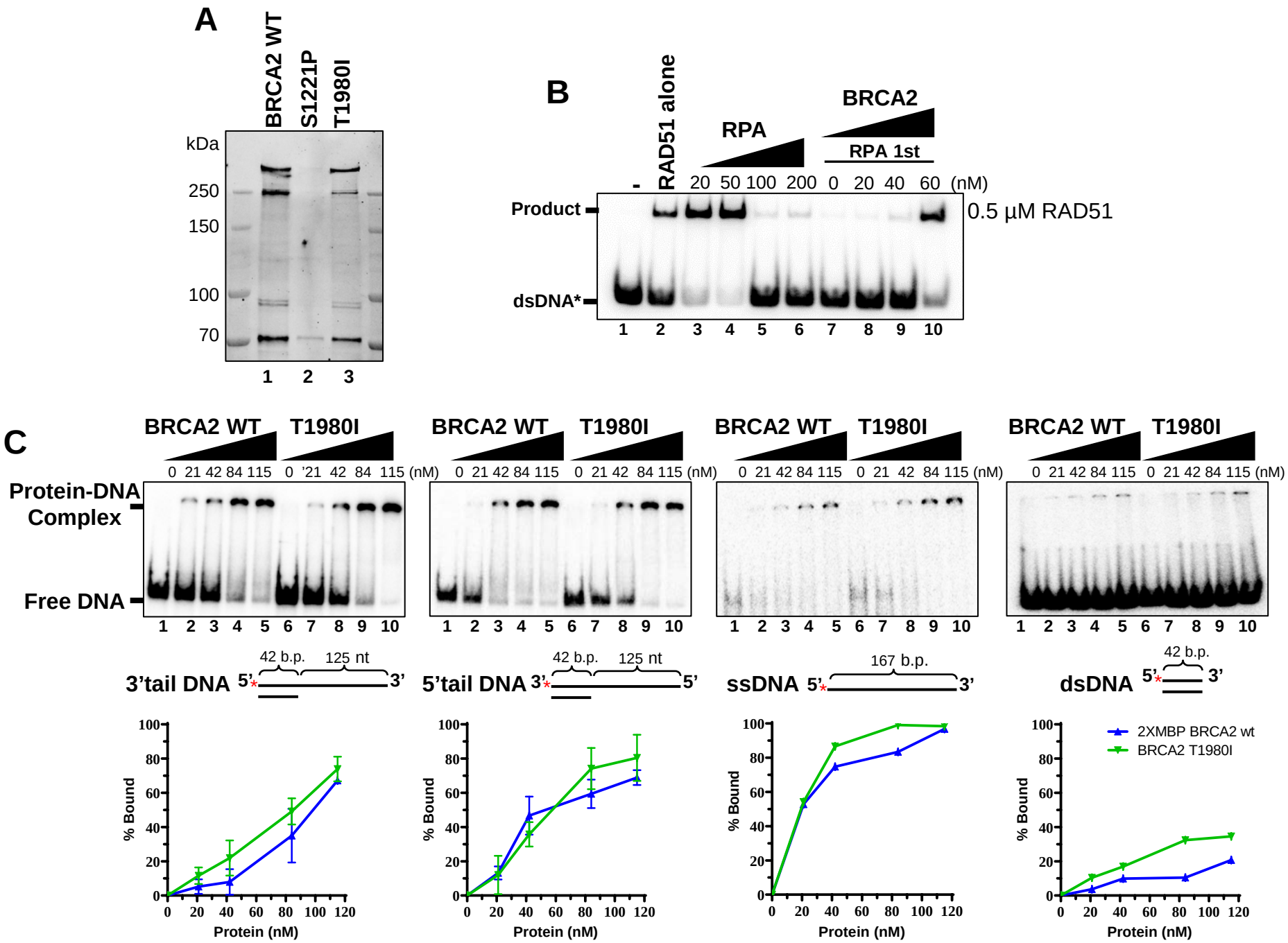

Supplementary Figure 7